Quantum Field Theory vs Reactor Anomaly

Vadim Naumov, Dmitry Shkirmanov

JINR, Dubna, Russia

May 2020

We thank Dmitry Naumov who participated in many stages of this research

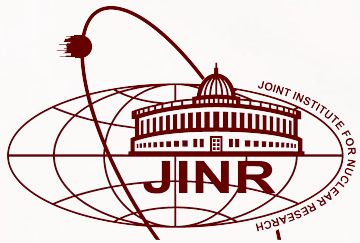

Motivation

- Reactor Antineutrino Anomaly (RAA) is a longstanding problem of neutrino physics.
- Most popular, resolution of the RAA is related to the hypothesis of a eV-scale sterile neutrino. But the latter seems to be in tension with many accelerator experiments and astrophysical/cosmological observations.
- Several years ago, we suggested another solution of the RAA[1] based on an extension of so-called Grimus-Stockinger theorem (GST)[2] describing the long-distance asymptotic behavior of the generalized ("macroscopic") neutrino propagator. The extended GST predicts a violation of the classical Inverse-Square Law (ISL) due to the NLO correction to the asymptotics.

---

[1] D. V. Naumov, V. A. Naumov, and D. S. Shkirmanov. *Phys. Part. Nucl.* **48**.1 (2017) 12. arXiv: 1507.04573 [hep-ph], D. V. Naumov, V. A. Naumov, and D. S. Shkirmanov. *Phys. Part. Nucl.* **48**.6 (2017) 1007

[2] V. A. Naumov and D. S. Shkirmanov. *Eur. Phys. J.* **C 73** (2013) 2627. arXiv: 1309.1011 [hep-ph], S. E. Korenblit and D. V. Taychenachev. *Mod. Phys. Lett.* **A 30** (2015) 1550074. arXiv: 1401.4031 [math-ph]

Motivation

- It has been shown that ISL violation (ISLV) could be responsible, at least in part, for the very short baseline (VSBL) reactor anomalies.
- Very recent VSBL data from **Nucifer**, **PROSPECT**, **STEREO**, **Neutrino-4**, and **DANSS** (yet preliminary) experiments as well as new improved measurements in the MBL experiments **Daya Bay**, **RENO**, and **Double Chooz** allows us to test the ISLV with much better confidence level.
- ★ **NOTE:** Recently, new reanalysis of the SBL and MBL data has been published[3]. We found several inconsistencies in the eprint and authors will update it soon. So we did not include their results into our analysis yet.

[3] J. M. Berryman and P. Huber. arXiv: 2005.01756 [hep-ph]

Table of Contents

RAA – State-of-the-art 2017 [4]

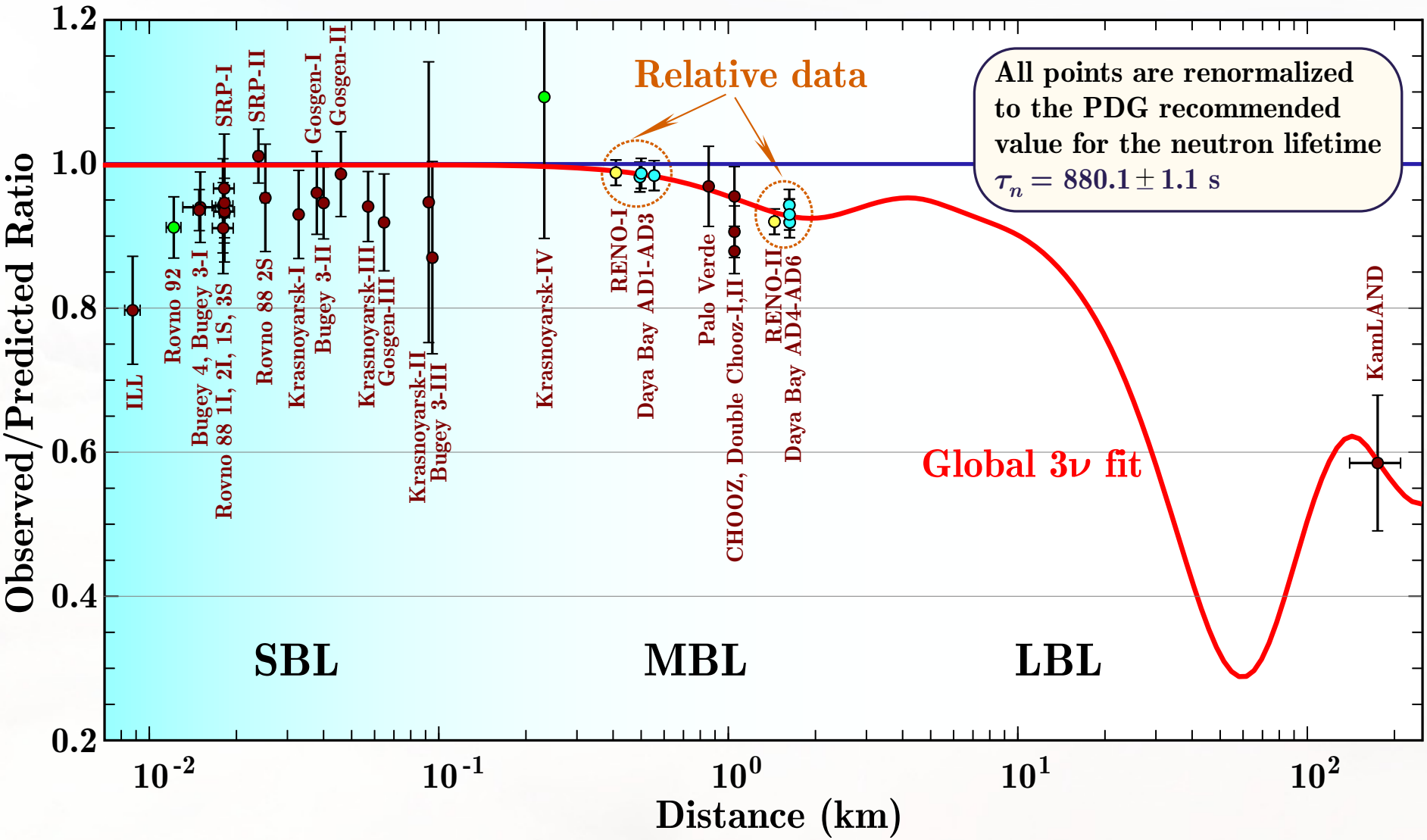

[4] D. V. Naumov, V. A. Naumov, and D. S. Shkirmanov. *Phys. Part. Nucl.* **48**.1 (2017) 12. arXiv: 1507.04573 [hep-ph].

Sterile neutrino? [5]

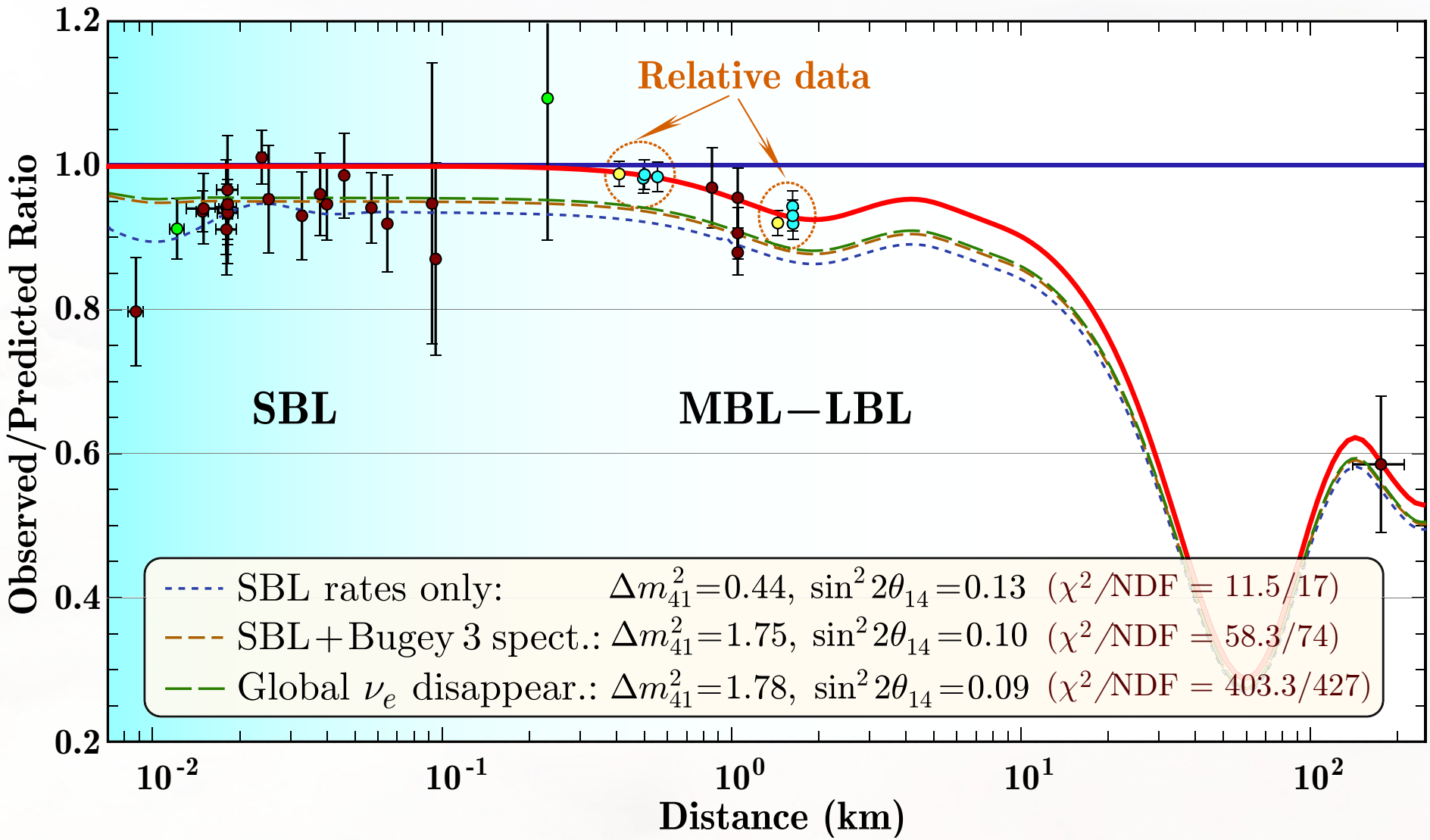

[5] The 3+1 fits are from J. Kopp *et al. JHEP* **05** (2013) 050. arXiv: 1303.3011v2 [hep-ph]

The antineutrino flux uncertainty

The anomaly may be more significant (or more uncertain!)

"In summary we find that the $\sim$ 30% forbidden transitions making up the aggregate fission spectra introduce a large uncertainty (at least 5%) in the predicted shape of the antineutrino flux emitted from reactors."[6]

[6] A. C. Hayes *et al. Phys. Rev. Lett.* **112** (2014) 202501. arXiv: 1309.4146 [nucl-th].

Flux normalization vs sterile neutrinos

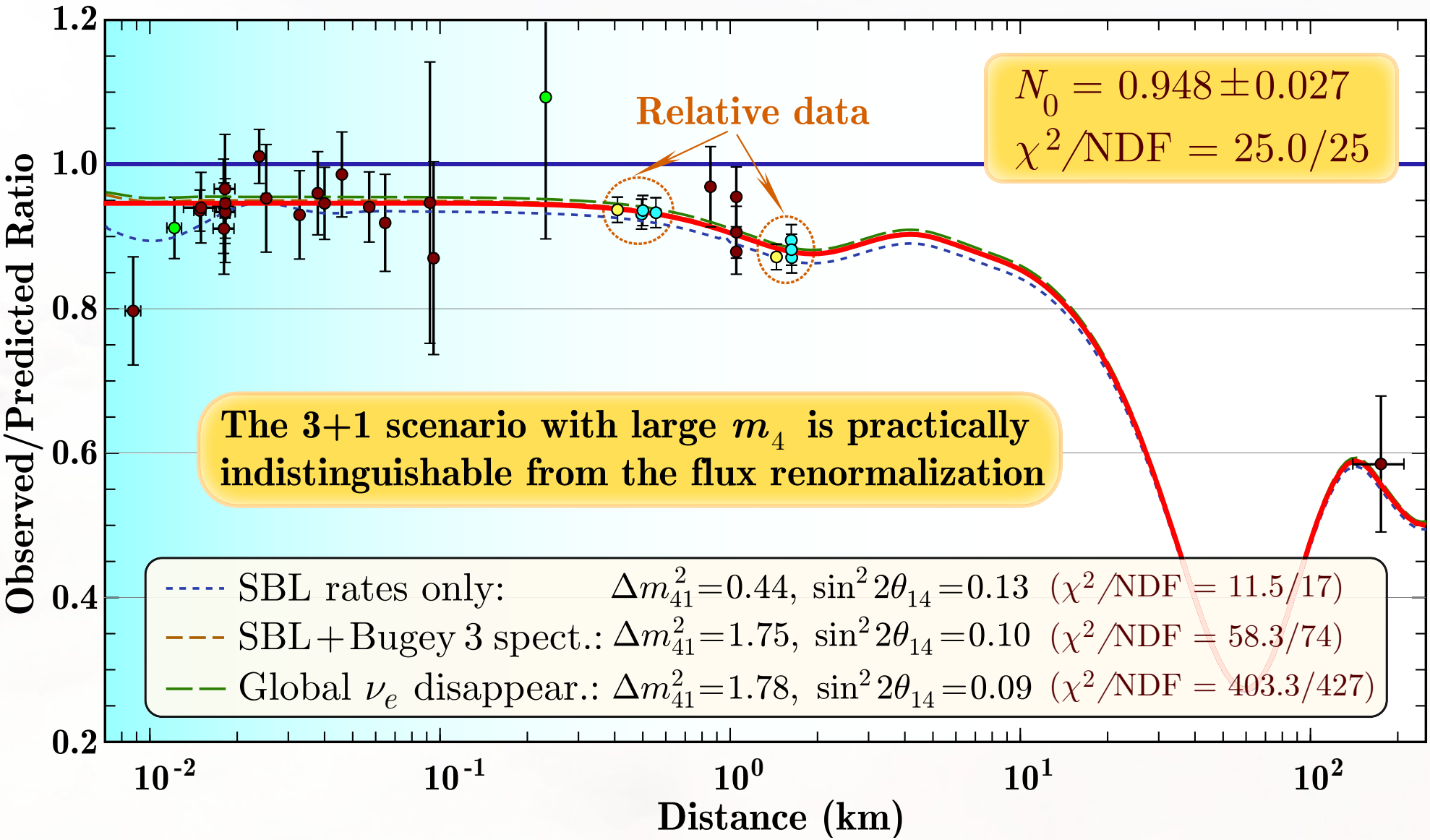

Inverse-Square Law violation

- According to the Inverse-square law, the neutrino event rate is inversely proportional to the squared distance between the neutrino source and detector:

$$dN_\nu \propto \frac{1}{L^2}.$$

  This simple geometrical theorem is a commonplace used “by default”.

- However! The Quantum Field theory of the neutrino oscillations predicts the inverse square law could be broken at short distances:

$$dN_\nu \propto \frac{1}{L^2}\left(1 - \frac{L_0^2}{L^2} + \dots\right)$$

Oscillation mechanism in quantum mechanics

Assumptions

- The flavor states are linear superposition of the massive states:

$$|\nu_\alpha\rangle = \sum_i V^*_{\alpha i} |\nu_i\rangle, \quad \alpha = e, \mu, \tau, \ldots$$

- All massive states have equal momenta: $\boldsymbol{p}_i = \boldsymbol{p}_\nu$.
- Neutrinos are **ultrarelativistic**, so $L \approx t$.

Schrödinger equation for the **massive** neutrino states reads:

$$i\frac{d}{dt}|\nu(t)\rangle_{\text{mass}} = \mathbf{H}_0|\nu(t)\rangle_{\text{mass}}, \quad \mathbf{H}_0 = \text{diag}(E_1, E_2, E_3, \ldots).$$

Equation for **flavor** states then follows from the above equation:

$$i\frac{d}{dt}|\nu(t)\rangle_{\text{flavor}} = \mathbf{V}^\dagger \mathbf{H}_0 \mathbf{V}|\nu(t)\rangle_{\text{flavor}}.$$

Standard QM formula for neutrino oscillations

The enumerated assumptions are sufficient to derive the nice and commonly accepted expression for the neutrino flavor transition probability:

The standard quantum mechanical formula

$$\mathcal{P}\left(\nu_\alpha \to \nu_\beta\right) \equiv \mathcal{P}_{\alpha\beta} = \sum_{ij} V_{\alpha i} V_{\beta j} V^*_{\alpha j} V^*_{\beta i} \exp\left(i \frac{m_i^2 - m_j^2}{2E} L\right)$$

Just this result is the basis for the "oscillation interpretation" of all current experiments with the natural and artificial neutrino and antineutrino beams.

The problem is that essentially all of these assumptions are incorrect...

Equal momentum assumption

- Massive neutrinos ν_i have by assumption equal momenta: $\boldsymbol{p}_i = \boldsymbol{p}_\nu$ ($i = 1, 2, 3$). This assumption is reference-frame (RF) dependent:

$$E'_i = \Gamma_{\boldsymbol{v}} \left[E_i - (\boldsymbol{v}\boldsymbol{p}_\nu) \right], \quad \boldsymbol{p}'_i = \boldsymbol{p}_\nu + \Gamma_{\boldsymbol{v}} \left[\frac{\Gamma_{\boldsymbol{v}} (\boldsymbol{v}\boldsymbol{p}_\nu)}{\Gamma_{\boldsymbol{v}} + 1} - E_i \right] \boldsymbol{v},$$

assuming that $m_i \neq m_j$ one can get:

$$\boldsymbol{p}'_i - \boldsymbol{p}'_j = \left(E'_j - E'_i \right) \boldsymbol{v} = \Gamma_{\boldsymbol{v}} \left(E_j - E_i \right) \boldsymbol{v} \neq 0.$$

- A similar objection exists against the alternative equal-energy assumption; in that case

$$E'_i - E'_j = \Gamma_{\boldsymbol{v}} \left(\boldsymbol{p}_j - \boldsymbol{p}_i \right) \boldsymbol{v} \neq 0.$$

Velocity difference

- As the massive neutrino components have the same momentum $\boldsymbol{p}_\nu$, their velocities are in fact different:

$$\boldsymbol{v}_i = \boldsymbol{p}_\nu / \sqrt{\boldsymbol{p}_\nu^2 + m_i^2} \quad \Longrightarrow \quad |\boldsymbol{v}_i - \boldsymbol{v}_j| \approx \Delta m_{ji}^2 / 2E_\nu^2.$$

- During the time T the neutrino ν_i travels the distance $L_i = |\boldsymbol{v}_i| T$.
- There must be a spread in distances of each neutrino pair

$$\delta L_{ij} = L_i - L_j \approx \Delta m_{ji}^2 \, L/2E_\nu^2, \quad \text{where} \quad L = cT = T,$$

$$L_{ij} = 4\pi E_\nu / \Delta m_{ij}^2 \quad \text{is the oscillation length}$$

Δm_{ji}^2	E_ν	L	L_{ij}	$\lvert\delta L_{ij}\rvert$
Δm_{23}^2	1 GeV	$2R_\oplus$	$0.1R_\oplus$	$\sim 10^{-12}$ cm
Δm_{21}^2	1 MeV	1 AU	$0.25R_\oplus$	$\sim 10^{-3}$ cm

Are $|\delta L_{ij}|$ sufficiently small to preserve the coherence?

Heavy neutrino

Question

Can light neutrinos oscillate into heavy ones or vice versa?

- The naive QM answer is Yes. Why not? If, at least, both ν_α (light) and ν_s (heavy) are ultrarelativistic one obtains the same formula for the oscillation probability since the QM formalism has no any limitation to the neutrino mass hierarchy.
- Possibility of such transitions is a basis for many speculations in astrophysics and cosmology
- But! Assume that the neutrino source is π_μ decay and $M > m_\pi$. the transition $\nu_\alpha \to \nu_s$ in the pion rest frame is forbidden by the energy conservation.

QFT approach

- Within the framework of the plane-wave formalism of Quantum Field Theory, the particles states are defined as Fock's states:

$$|\boldsymbol{k}, s\rangle = \sqrt{2E_{\boldsymbol{k}}}\, a^{\dagger}_{\boldsymbol{k}s}|0\rangle. \tag{1}$$

- The Fock states have no information about the particle coordinate.
- ★ To introduce dependence on the coordinate one needs to build a wave packet that is superposition of the Fock states:

$$|\boldsymbol{p}, s, x\rangle = \int \frac{d\boldsymbol{k}\, \phi(\boldsymbol{k}, \boldsymbol{p}) e^{i(k-p)x}}{(2\pi)^3 2E_{\boldsymbol{k}}} |\boldsymbol{k}, s\rangle, \quad \phi(\boldsymbol{k}, \boldsymbol{p}) \overset{\text{PWL}}{\longmapsto} (2\pi)^3 2E_{\boldsymbol{p}} \delta(\boldsymbol{k} - \boldsymbol{p}).$$

- The amplitude is constructed as follows:

$$\langle \mathbf{out}|\mathbb{S}|\mathbf{in}\rangle \left(\langle \mathbf{in}|\mathbf{in}\rangle\langle \mathbf{out}|\mathbf{out}\rangle\right)^{-1/2} \overset{\text{def}}{=} \mathcal{A}_{\beta\alpha}.$$

QFT approach

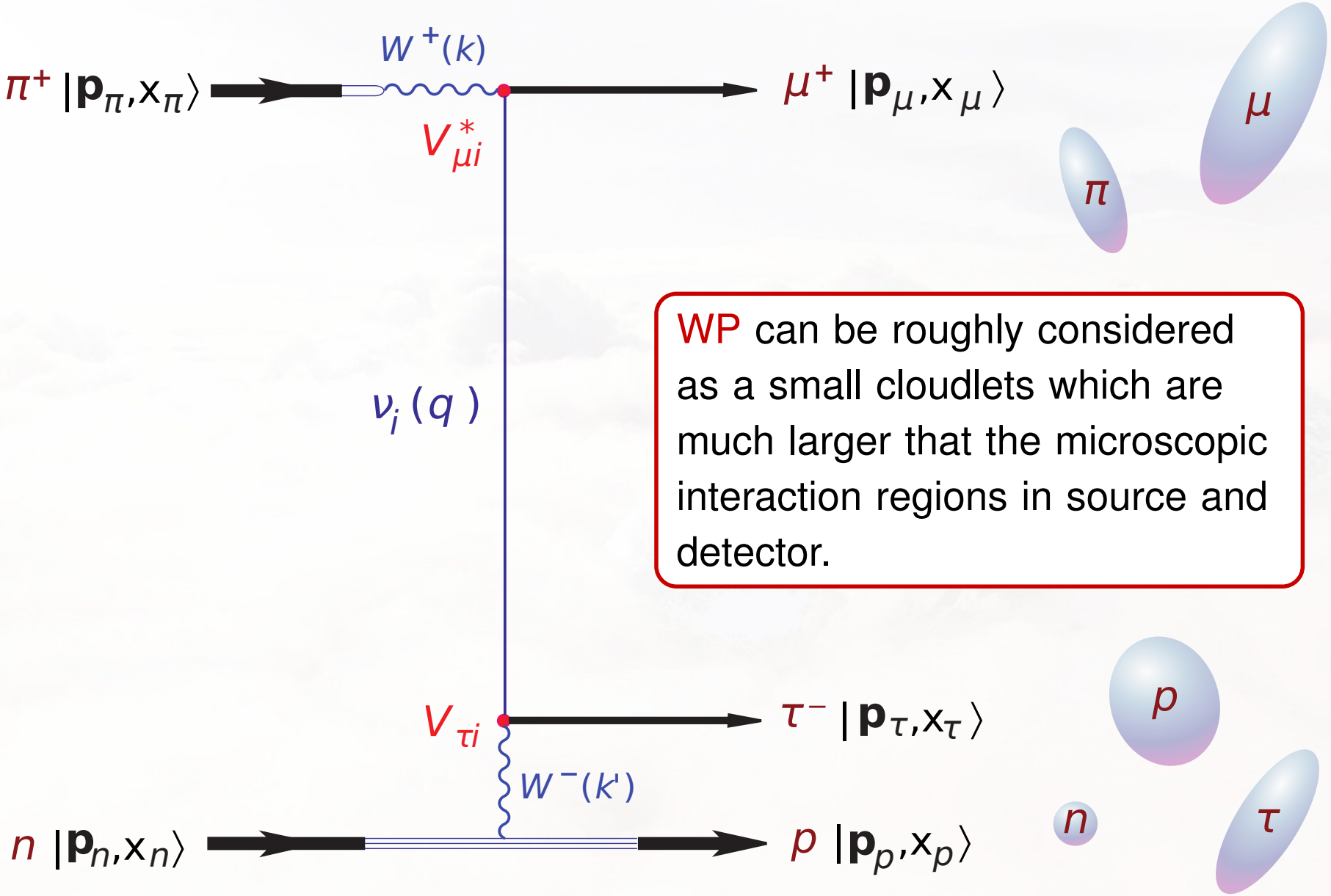

WP can be roughly considered as a small cloudlets which are much larger that the microscopic interaction regions in source and detector.

Neutrino event rate

- Within the QFT approach the neutrino event rate has the form[7]:

$$\frac{dN}{d\tau} = \frac{1}{V_{\mathcal{D}} V_{\mathcal{S}}} \int_{V_{\mathcal{S}}} d\boldsymbol{x} \int_{V_{\mathcal{D}}} d\boldsymbol{y} \int d\mathfrak{F}_{\nu} \int d\sigma_{\nu\mathcal{D}} \mathcal{P}_{\alpha\beta}\left(E_{\nu}, |\boldsymbol{y}-\boldsymbol{x}|\right). \tag{2}$$

  τ is the detector exposure time, E_{ν} is the neutrino energy, $V_{\mathcal{S}}$ and $V_{\mathcal{D}}$ are the spatial volumes of source $\mathcal{S}$ and detector $\mathcal{D}$ "devices".

- The theory predicts that the neutrino flux behaves according to the classical inverse-square law (ISL):

$$d\mathfrak{F}_{\nu} \propto |\boldsymbol{y}-\boldsymbol{x}|^{-2}, \tag{3}$$

- ISL is derived for the asymptotically long distances, $|\boldsymbol{y}-\boldsymbol{x}| \to \infty$.

[7] D. V. Naumov and V. A. Naumov. *J. Phys.* **G 37** (2010) 105014. arXiv: 1008.0306v2 [hep-ph]

The origins of the ISL

The L dependence of the amplitude is defined by the external WP-modified ν propagator:

$$\int \frac{d^4q}{(2\pi)^4} \frac{\widetilde{\delta}_s(q-q_s)\widetilde{\delta}_d(q+q_d)(\hat{q}+m)e^{-iqX}}{q^2-m^2+i\epsilon},$$

where $\widetilde{\delta}_{s,d}$ are "smeared" δ functions, responsible for approximate 4-momentum conservation in the vertices, $X = (T, \boldsymbol{L})$; $q_{s,d}$ are the 4-momentum transfers in the source/detector.

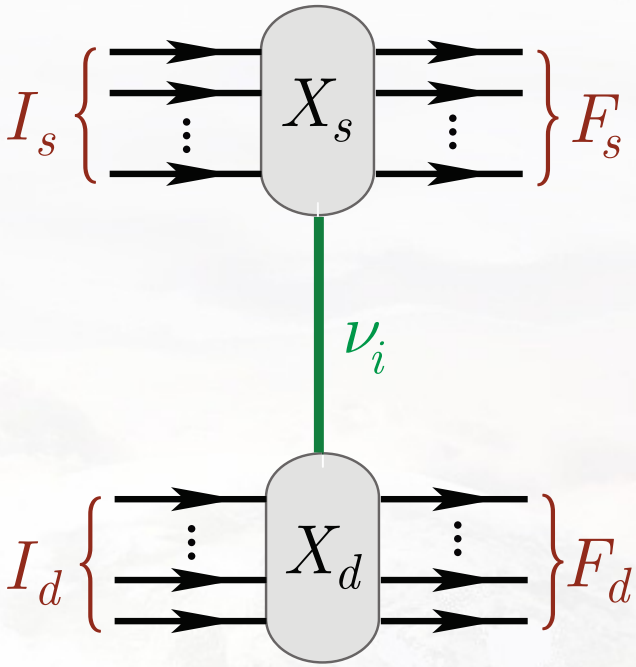

- Extended Grimus-Stockinger theorem[8]: For $\Phi(\boldsymbol{q}) \in S(\mathbb{R}^3)$ and $\omega > 0$

$$J(L,\omega) \stackrel{\text{def}}{=} \int \frac{d\boldsymbol{q}}{(2\pi)^3} \frac{\Phi(\boldsymbol{q})e^{i\boldsymbol{q}\boldsymbol{L}}}{\boldsymbol{q}^2-\omega^2-i\epsilon} = \frac{e^{i\omega L}}{4\pi L}\sum_{k\geqslant 0}\frac{(-i)^k\left[D_k\Phi(\boldsymbol{q})\right]_{\boldsymbol{q}=\omega\boldsymbol{l}}}{L^k}, \quad L\to\infty.$$

Here $L = |\boldsymbol{L}|$, $\boldsymbol{l} = \boldsymbol{L}/L$, and D_k are recurrently defined differential operators.

[8] V. A. Naumov and D. S. Shkirmanov. *Eur. Phys. J.* **C 73** (2013) 2627. arXiv: 1309.1011 [hep-ph]. Below, this paper will be referred to as **[NS-2013]**.

Extended Grimus-Stockinger theorem

The lowest order operators D_k are

$$D_0 = 1,$$

$$D_1 = \frac{\omega}{2}\left[\nabla_q^2 - (l\nabla_q)^2\right] - (l\nabla_q),$$

$$D_2 = \frac{\omega^2}{8}\left[\nabla_q^2 - (l\nabla_q)^2\right]^2 - \omega(l\nabla_q)\left[\nabla_q^2 - (l\nabla_q)^2\right] - \frac{1}{2}\left[\nabla_q^2 - 3(l\nabla_q)^2\right].$$

$$D_3 = \frac{\omega^3}{48}\left[\nabla_q^2 - (l\nabla_q)^2\right]^3 - \frac{3\omega^2}{8}(l\nabla_q)\left[\nabla_q^2 - (l\nabla_q)^2\right]^2 - \frac{3\omega}{8}\left[\nabla_q^2 - (l\nabla_q)^2\right] \times \left[\nabla_q^2 - 5(l\nabla_q)^2\right] + \frac{1}{2}(l\nabla_q)\left[3\nabla_q^2 - 5(l\nabla_q)^2\right],$$

$$D_4 = \frac{\omega^4}{384}\left[\nabla_q^2 - (l\nabla_q)^2\right]^4 - \frac{\omega^3}{12}(l\nabla_q)\left[\nabla_q^2 - (l\nabla_q)^2\right]^3 - \frac{\omega^2}{8}\left[\nabla_q^2 - (l\nabla_q)^2\right] \times \left[\nabla_q^2 - 7(l\nabla_q)^2\right] - \frac{\omega}{2}(l\nabla_q)\left[\nabla_q^2 - (l\nabla_q)^2\right]\left[3\nabla_q^2 - 7(l\nabla_q)^2\right] + \frac{1}{8}\left[3\nabla_q^4 - 30\nabla_q^2(l\nabla_q)^2 + 35(l\nabla_q)^4\right].$$

How probability depends on distance

- After accomplishing (complicated) integration in the propagator over q_0, one finds out the modulus squared amplitude, which is proportional to

$$|J(-\boldsymbol{L},\omega)|^2 = \sum_{k=1}^{\infty}\sum_{n=0}^{2(k-1)} \frac{C_{kn}\omega^n}{L^{2k}} = \frac{1}{L^2}\left[\Phi^2(\omega \boldsymbol{l}) + \sum_{k=1}^{\infty}\sum_{n=0}^{2k} \frac{C_{k+1,n}\omega^n}{L^{2k}}\right].$$

- The series describes deviation from the inverse-square law.
- The coefficients C_{kn} can be recursively found, e.g.

$$C_{10} = f^2;\ \ C_{20} = ff_{20} - 2ff_{02} + f_{01}^2,\ \ C_{21} = f_{20}f_{01} - 2ff_{21},\ \ C_{22} = \frac{1}{4}\left(f_{20}^2 - ff_{40}\right);$$

$$C_{30} = \left(\frac{3}{4}f_{40} - 6f_{22} + 2f_{04}\right) f + \left(3f_{21} - 2f_{03}\right) f_{01} + \left(f_{02} - \frac{1}{2}f_{20}\right)^2,$$

$$C_{31} = \left(4f_{23} - 3f_{41}\right) f + \left(\frac{1}{2}f_{20} + 2f_{02}\right) f_{21} + 3\left(\frac{1}{4}f_{40} - f_{22}\right) f_{01} - f_{20}f_{03},$$

$$C_{32} = \frac{1}{4}\left(f_{40} - 6f_{22}\right) f_{20} + \frac{1}{4}f_{02}f_{40} + \frac{1}{4}\left(6f_{42} - f_{60}\right) f - \frac{3}{4}f_{01}f_{41} + f_{21}^2, \ldots$$

$$f_{ij} = \left(\boldsymbol{l}\times\boldsymbol{\nabla}_{\boldsymbol{q}}\right)^i \left(-\boldsymbol{l}\boldsymbol{\nabla}_{\boldsymbol{q}}\right)^j \Phi(\boldsymbol{q})\Big|_{\boldsymbol{q}=\omega\boldsymbol{l}}, \quad f \equiv f_{00} = \Phi(\omega\boldsymbol{l}).$$

The flux

- After several pages of calculations we can find out how does the neutrino flux depend on distance:

$$d\mathfrak{F}_\nu \propto \frac{1}{|\boldsymbol{y}-\boldsymbol{x}|^2}\left[1+\sum_{n\geqslant 1}\frac{\mathfrak{C}_n}{|\boldsymbol{y}-\boldsymbol{x}|^{2n}}\right], \tag{4}$$

- the leading term of the series describes deviation from Inverse-square law:

$$\mathfrak{C}_1 = \frac{1}{f^2}\left[f_{01}^2 + f\left(f_{20}-2f_{02}\right) + \left(f_{20}f_{01}-2ff_{21}\right)E_\nu + \frac{1}{4}\left(f_{20}^2-ff_{40}\right)E_\nu^2\right].$$

$$f_{ij} = \left(\boldsymbol{l}\times\boldsymbol{\nabla}_{\boldsymbol{q}}\right)^i\left(-\boldsymbol{l}\boldsymbol{\nabla}_{\boldsymbol{q}}\right)^j\Phi(\boldsymbol{q})\Big|_{\boldsymbol{q}=\omega\boldsymbol{l}}, \quad f\equiv f_{00}=\Phi(\omega\boldsymbol{l}).$$

- IMPORTANT! Using the explicit form of $\Phi(\boldsymbol{q})$ in the so-called CRGP[9] wave-packet model, it is proved that in the physical region

$$\mathfrak{C}_1 = -E_\nu^2\sigma_{\text{eff}}^{-4} < 0.$$ Details

[9] D. V. Naumov and V. A. Naumov. *J. Phys.* **G 37** (2010) 105014. arXiv: 1008.0306v2 [hep-ph].

ISL Violation: the summary

- By applying the extended Grimus-Stockinger theorem, it is proved that the neutrino event rate in the detector is proportional to the factor

$$dN_\nu \propto \frac{1}{L^2}\left[1 - \frac{L_0^2}{L^2} + \dots\right]. \tag{5}$$

- The leading-order ISLV correction is negative and L_0 is an energy dependent parameter of dimension of length:

$$L_0 \sim \langle E_\nu \sigma_{\text{eff}}^{-2}(E_\nu)\rangle \approx 20 \left\langle \left(\frac{E_\nu}{1\ \text{MeV}}\right)\left[\frac{\sigma_{\text{eff}}(E_\nu)}{1\ \text{eV}}\right]^{-2}\right\rangle \text{cm}. \tag{6}$$

The ISL violation effect might be observable.

Our reanalysis of the reactor data.

- A new careful analysis of the systematic error correlations in the reactor data set is performed. As a result the errors in general differ from those adopted by Mention *et al.*[10] and Zhang *et al.*[11] and are closer to those adopted by Kopp *et al.*[12].
  - — correlated groups are re-ordered.
  - — correlations are revisited.
- Some omitted data are added.
- New (recommended in RPP-2018) neutron lifetime $\tau_n = 880.2 \pm 1.0$ s is accounted for, instead of $\tau_n = 885.7$ s used in the mentioned analyses (this shifts down all the ratios by about 0.6%).

[10] G. Mention *et al. Phys. Rev.* **D 83** (2011) 073006. arXiv: 1101.2755 [hep-ex].

[11] C. Zhang, X. Qian, and P. Vogel. *Phys. Rev.* **D 87** (2013) 073018. arXiv: 1303.0900 [nucl-ex].

[12] J. Kopp *et al. JHEP* **05** (2013) 050. arXiv: 1303.3011v2 [hep-ph]. Note that the "Observed/Predicted" ratios listed in that paper are systematically (1 to 1.2%) smaller than ours.

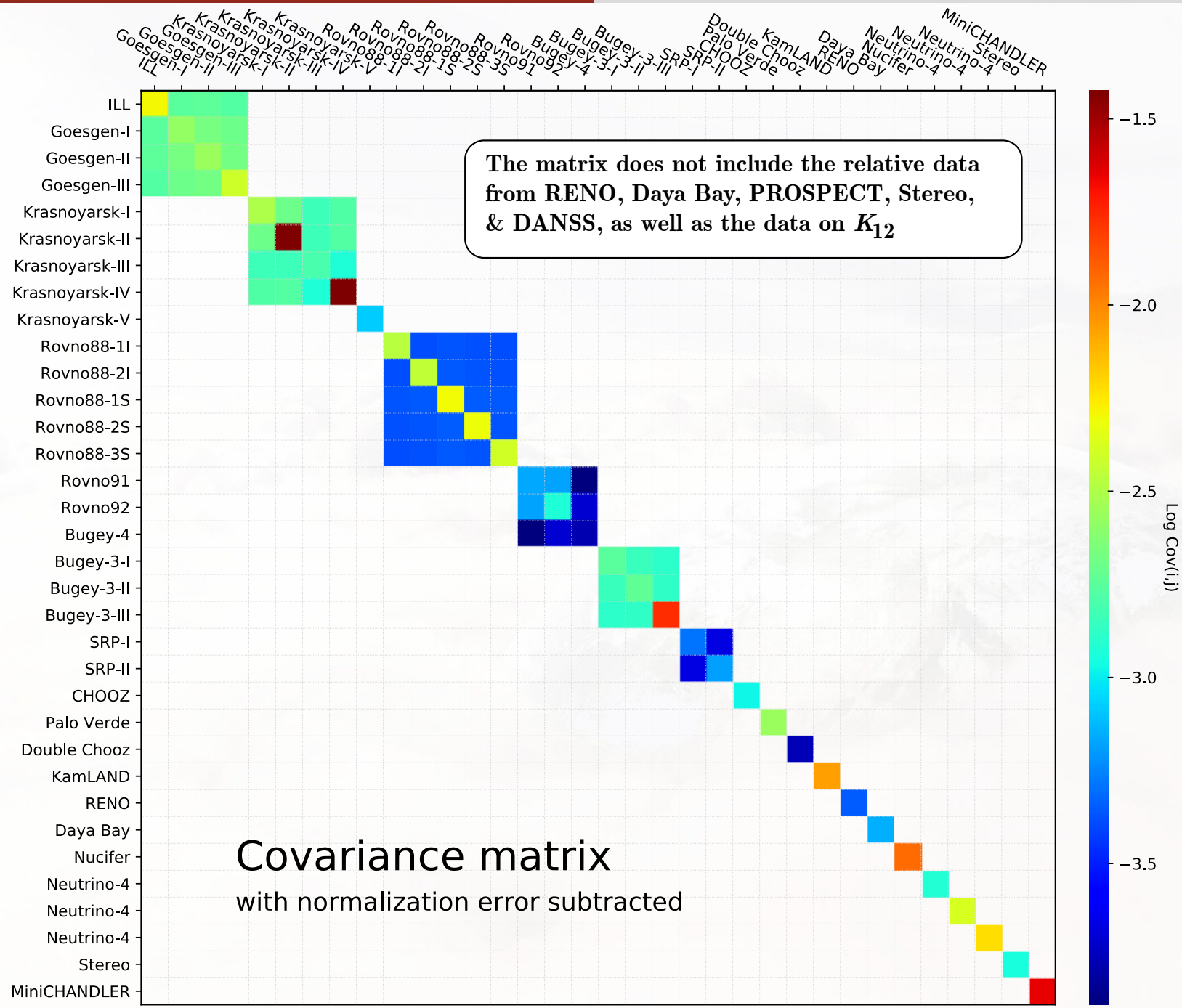
ILL
Goesgen-I
Goesgen-II
Goesgen-III
Krasnoyarsk-I
Krasnoyarsk-II
Krasnoyarsk-III
Krasnoyarsk-IV
Krasnoyarsk-V
Rovno88-1I
Rovno88-2I
Rovno88-1S
Rovno88-2S
Rovno88-3S
Rovno91
Rovno92
Bugey-4
Bugey-3-I
Bugey-3-II
Bugey-3-III
SRP-I
SRP-II
CHOOZ
Palo Verde
Double Chooz
KamLAND
RENO
Daya Bay
Nucifer
Neutrino-4
Neutrino-4
Neutrino-4
Stereo
MiniCHANDLER
The matrix does not include the relative data from RENO, Daya Bay, PROSPECT, Stereo, & DANSS, as well as the data on K_{12}
Covariance matrix
with normalization error subtracted
−1.5
−2.0
−2.5
−3.0
−3.5
Log Cov(i,j)

Comparison of models for $\overline{\nu}_e$ spectra

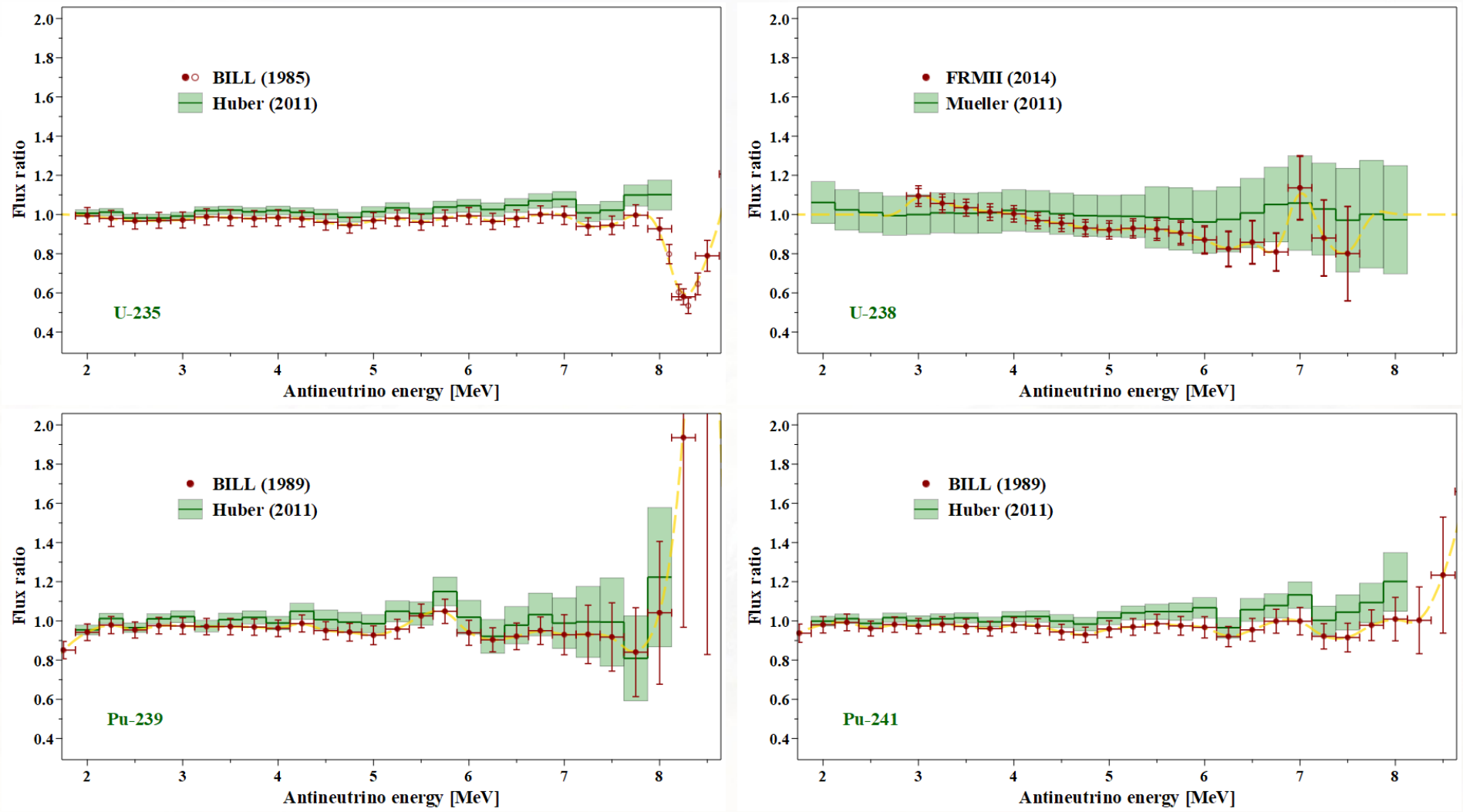

The spectra are normalized to the parametrization of Mueller's spectra[13].

[13] Th A. Mueller *et al. Phys. Rev.* **C 83** (2011) 054615. arXiv: 1101.2663 [hep-ex].

Comparison of models for $\overline{\nu}_e$ spectra

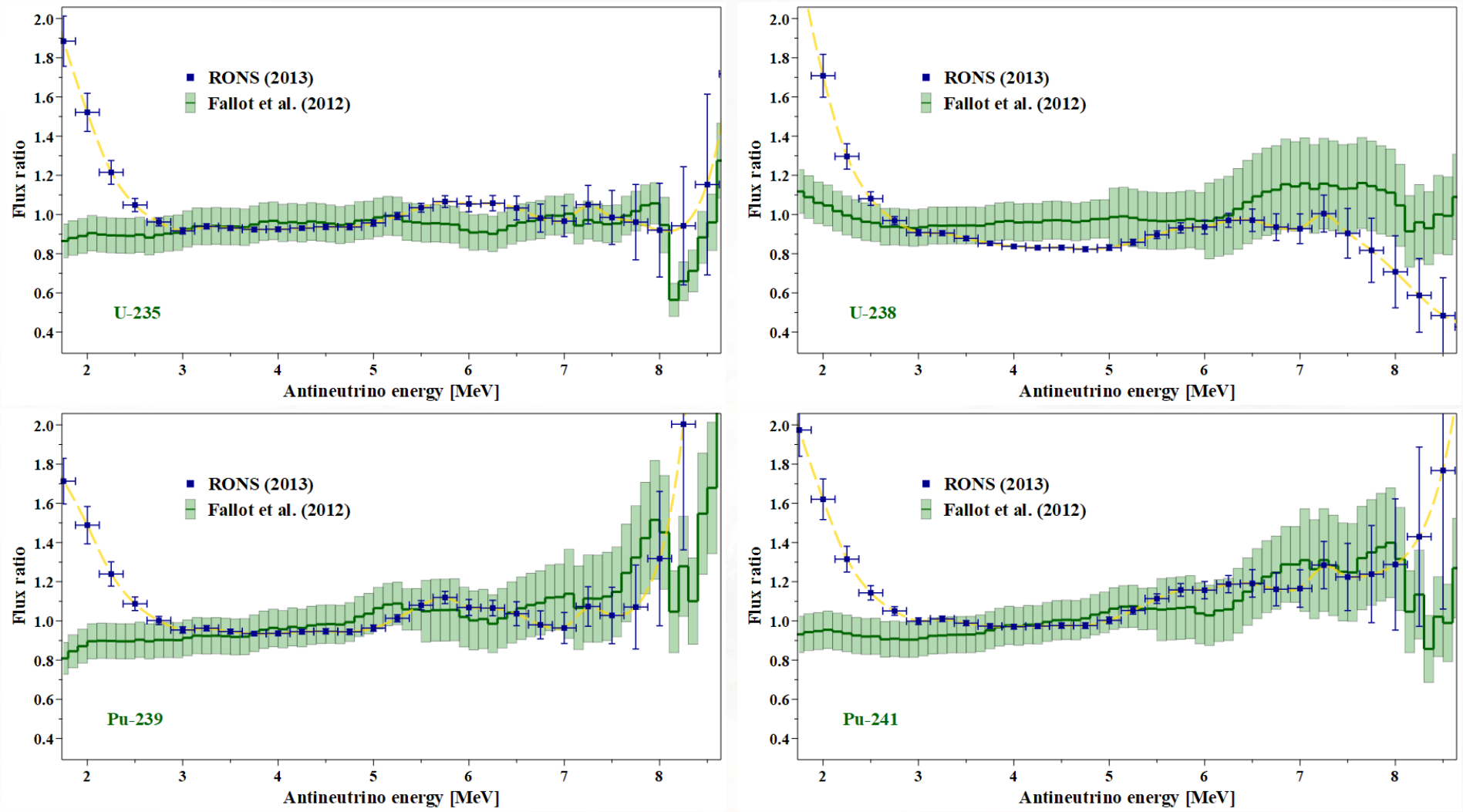

The spectra are normalized to the parametrization of Mueller's spectra[14].

[14] Th A. Mueller *et al. Phys. Rev.* **C 83** (2011) 054615. arXiv: 1101.2663 [hep-ex].

ISL violation

Theoretical model:

$$T(L; N_0, L_0) = N_0 \cdot \langle P^{3\nu}_{\text{surv}}(L) \rangle \cdot \left(1 - \frac{L_0^2}{L^2}\right). \tag{7}$$

N_0 is a free normalization parameter and

$$\langle P_{\text{surv}}(L) \rangle = \frac{\int_0^\infty dE \sum_k f_k P^{3\nu}_{\text{surv}}(L, E) \sigma(E) S_k(E)}{\int_0^\infty dE \sum_k f_k \sigma(E) S_k(E)}, \tag{8}$$

f_k is the fraction of main fissile isotope contributing to the $\overline{\nu}_e$ flux with a spectrum in energy $S_k(E)$[15], $\sigma(E)$ is the IBD cross section[16]
$P^{3\nu}_{\text{surv}}(L, E)$ is the $\overline{\nu}_e$ survival probability in the standard 3ν mixing scheme:

$$P^{3\nu}_{\text{surv}}(L, E) = 1 - \sin^2(2\theta_{13}) \left(\cos^2\theta_{12} \sin^2\Delta_{31} + \sin^2\theta_{12} \sin^2\Delta_{32}\right)$$
$$- \cos^4\theta_{13} \sin^2(2\theta_{12}) \sin^2\Delta_{21}, \qquad \Delta_{ij} = 1.267 \Delta m^2_{ij} L/E.$$

[15] Th A. Mueller *et al. Phys. Rev.* **C 83** (2011) 054615. arXiv: 1101.2663 [hep-ex]
[16] A. N. Ivanov *et al. Phys. Rev.* **C 88** (2013) 055501. arXiv: 1306.1995v2 [hep-ph]

Neutrino parameters used in the analysis [NuFIT 4.0 (2018)]

		Normal Ordering (best fit)		Inverted Ordering ($\Delta\chi^2 = 4.7$)	
		bfp $\pm 1\sigma$	3σ range	bfp $\pm 1\sigma$	3σ range
without SK atmospheric data	$\sin^2\theta_{12}$	$0.310^{+0.013}_{-0.012}$	$0.275 \to 0.350$	$0.310^{+0.013}_{-0.012}$	$0.275 \to 0.350$
	$\theta_{12}/^\circ$	$33.82^{+0.78}_{-0.76}$	$31.61 \to 36.27$	$33.82^{+0.78}_{-0.76}$	$31.61 \to 36.27$
	$\sin^2\theta_{23}$	$0.580^{+0.017}_{-0.021}$	$0.418 \to 0.627$	$0.584^{+0.016}_{-0.020}$	$0.423 \to 0.629$
	$\theta_{23}/^\circ$	$49.6^{+1.0}_{-1.2}$	$40.3 \to 52.4$	$49.8^{+1.0}_{-1.1}$	$40.6 \to 52.5$
	$\sin^2\theta_{13}$	$0.02241^{+0.00065}_{-0.00065}$	$0.02045 \to 0.02439$	$0.02264^{+0.00066}_{-0.00066}$	$0.02068 \to 0.02463$
	$\theta_{13}/^\circ$	$8.61^{+0.13}_{-0.13}$	$8.22 \to 8.99$	$8.65^{+0.13}_{-0.13}$	$8.27 \to 9.03$
	$\delta_{CP}/^\circ$	215^{+40}_{-29}	$125 \to 392$	284^{+27}_{-29}	$196 \to 360$
	$\frac{\Delta m^2_{21}}{10^{-5}\ \mathrm{eV}^2}$	$7.39^{+0.21}_{-0.20}$	$6.79 \to 8.01$	$7.39^{+0.21}_{-0.20}$	$6.79 \to 8.01$
	$\frac{\Delta m^2_{3\ell}}{10^{-3}\ \mathrm{eV}^2}$	$+2.525^{+0.033}_{-0.032}$	$+2.427 \to +2.625$	$-2.512^{+0.034}_{-0.032}$	$-2.611 \to -2.412$
		Normal Ordering (best fit)		Inverted Ordering ($\Delta\chi^2 = 9.3$)	
		bfp $\pm 1\sigma$	3σ range	bfp $\pm 1\sigma$	3σ range
with SK atmospheric data	$\sin^2\theta_{12}$	$0.310^{+0.013}_{-0.012}$	$0.275 \to 0.350$	$0.310^{+0.013}_{-0.012}$	$0.275 \to 0.350$
	$\theta_{12}/^\circ$	$33.82^{+0.78}_{-0.76}$	$31.61 \to 36.27$	$33.82^{+0.78}_{-0.75}$	$31.62 \to 36.27$
	$\sin^2\theta_{23}$	$0.582^{+0.015}_{-0.019}$	$0.428 \to 0.624$	$0.582^{+0.015}_{-0.018}$	$0.433 \to 0.623$
	$\theta_{23}/^\circ$	$49.7^{+0.9}_{-1.1}$	$40.9 \to 52.2$	$49.7^{+0.9}_{-1.0}$	$41.2 \to 52.1$
	$\sin^2\theta_{13}$	$0.02240^{+0.00065}_{-0.00066}$	$0.02044 \to 0.02437$	$0.02263^{+0.00065}_{-0.00066}$	$0.02067 \to 0.02461$
	$\theta_{13}/^\circ$	$8.61^{+0.12}_{-0.13}$	$8.22 \to 8.98$	$8.65^{+0.12}_{-0.13}$	$8.27 \to 9.03$
	$\delta_{CP}/^\circ$	217^{+40}_{-28}	$135 \to 366$	280^{+25}_{-28}	$196 \to 351$
	$\frac{\Delta m^2_{21}}{10^{-5}\ \mathrm{eV}^2}$	$7.39^{+0.21}_{-0.20}$	$6.79 \to 8.01$	$7.39^{+0.21}_{-0.20}$	$6.79 \to 8.01$
	$\frac{\Delta m^2_{3\ell}}{10^{-3}\ \mathrm{eV}^2}$	$+2.525^{+0.033}_{-0.031}$	$+2.431 \to +2.622$	$-2.512^{+0.034}_{-0.031}$	$-2.606 \to -2.413$

ISLV, Spectrum type = Mueller

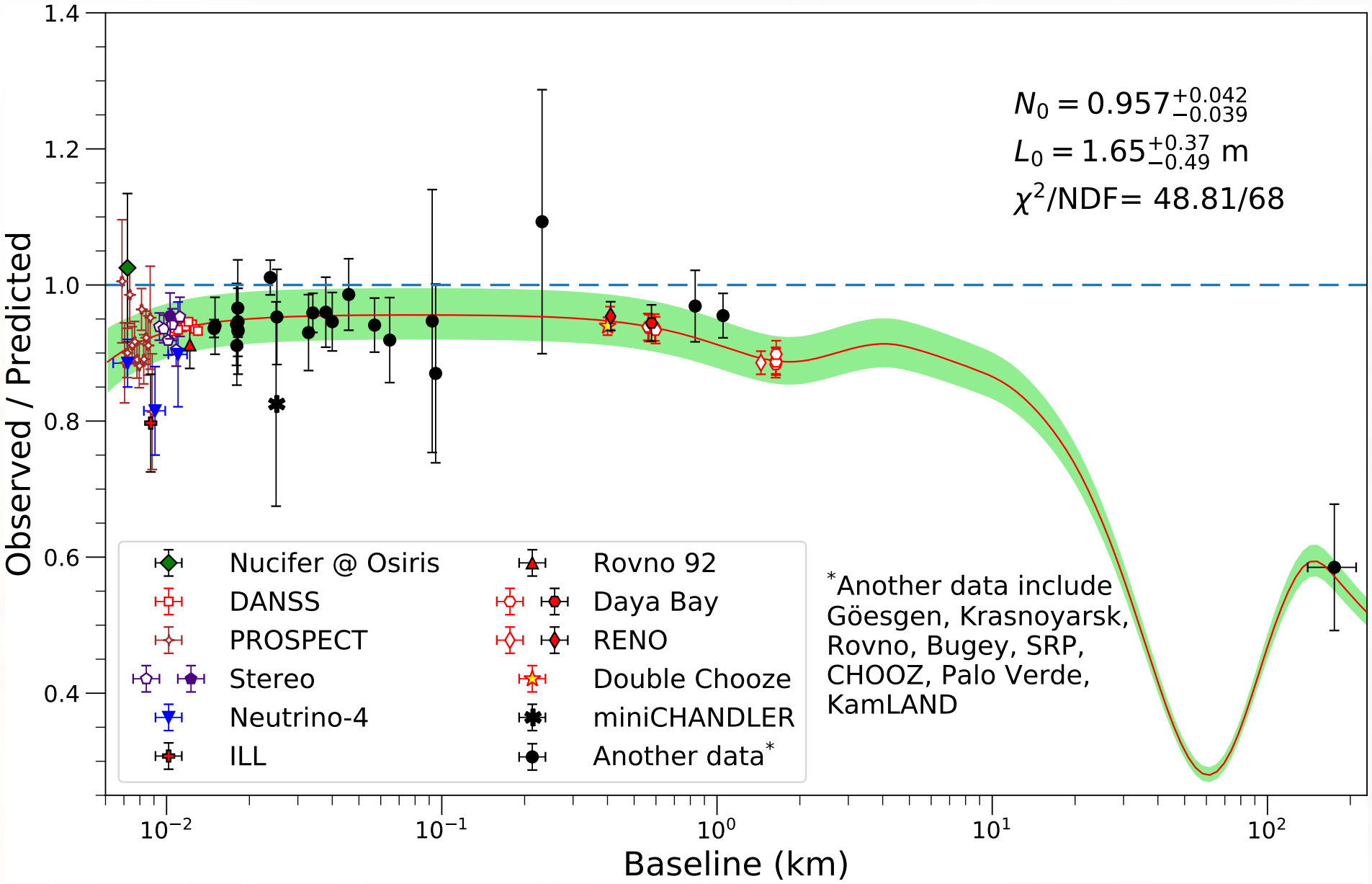

Effect of isotope composition

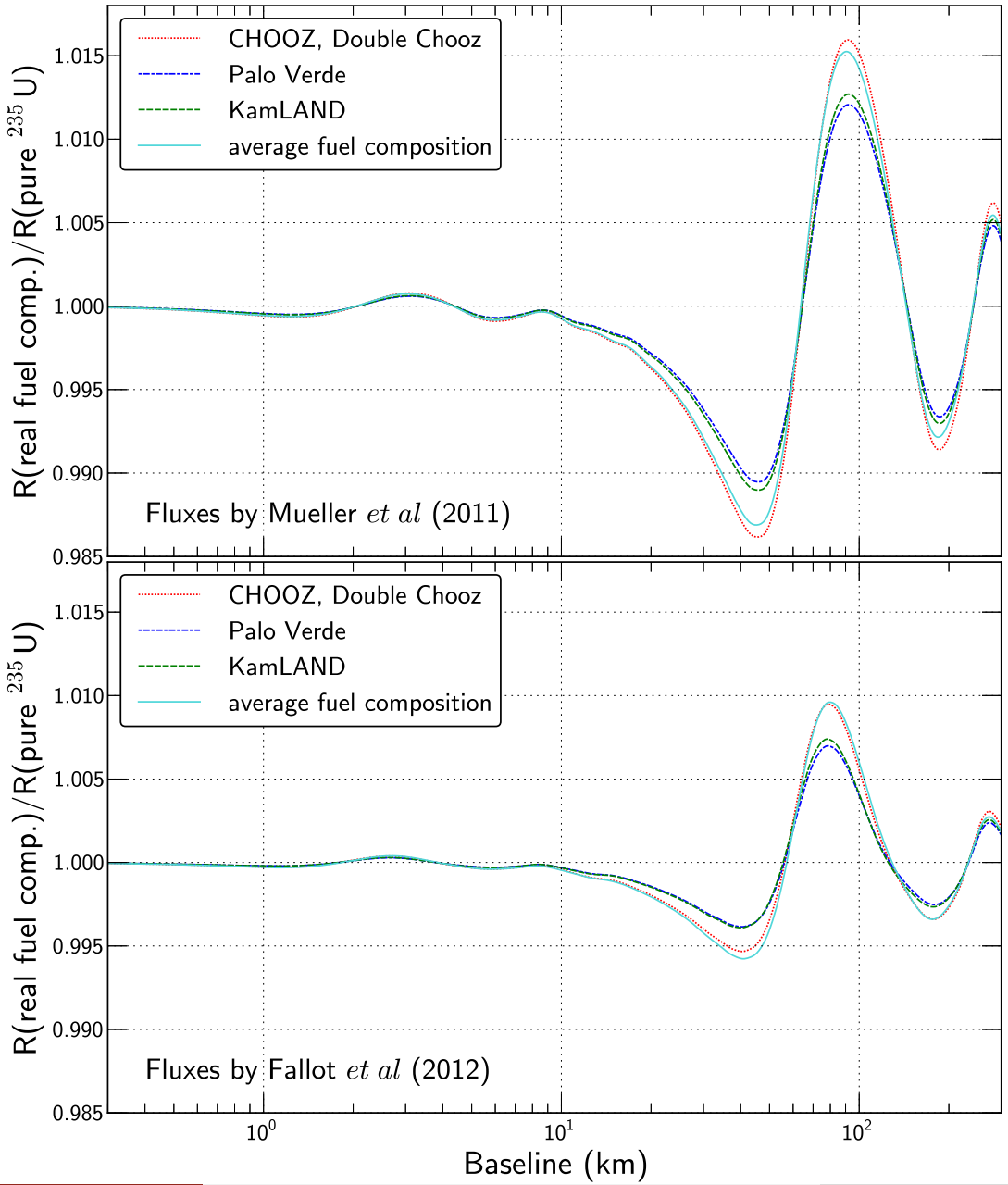

ISLV, Spectrum type = Fallot

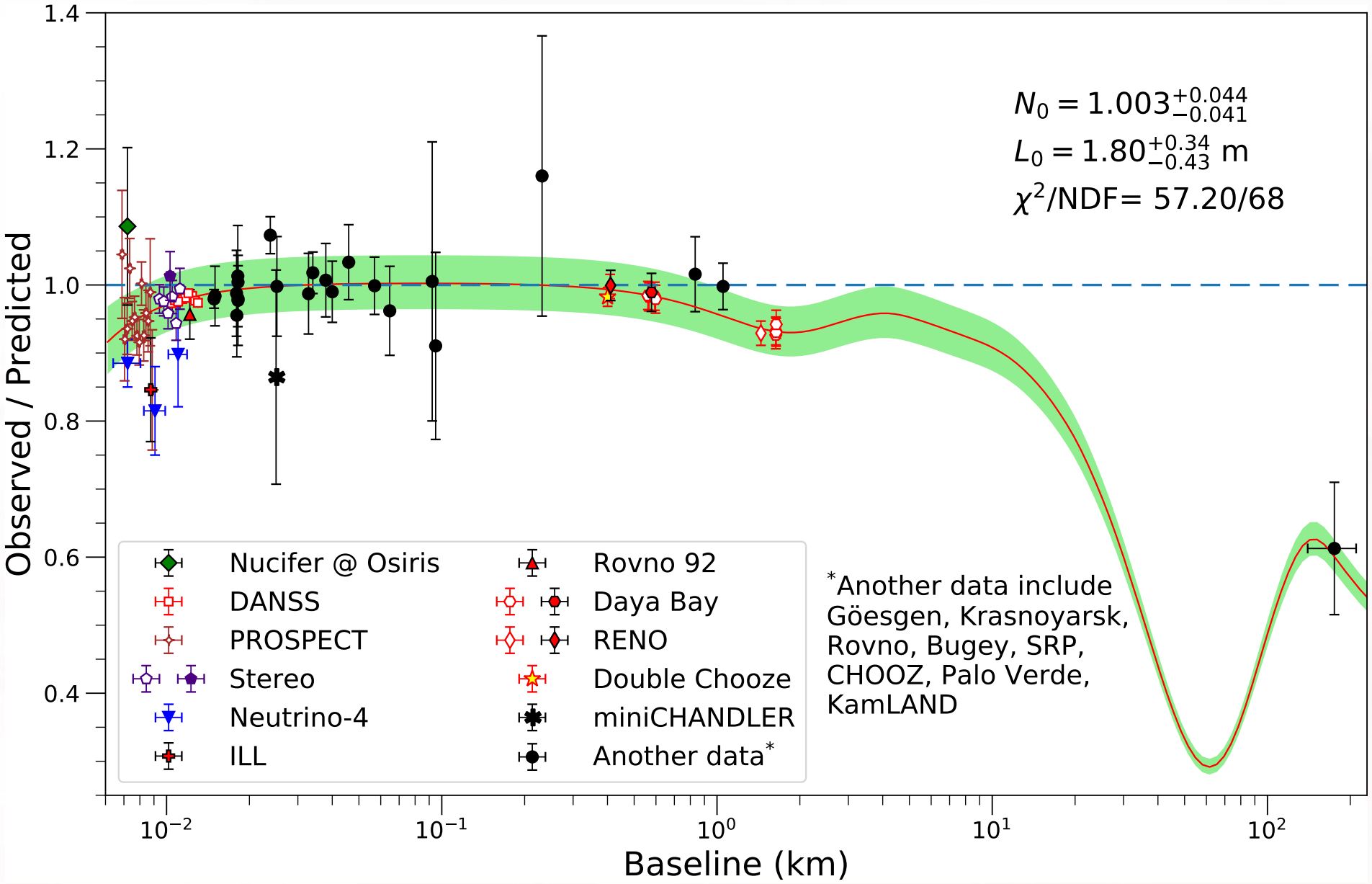

ISLV, Spectrum type = Mueller

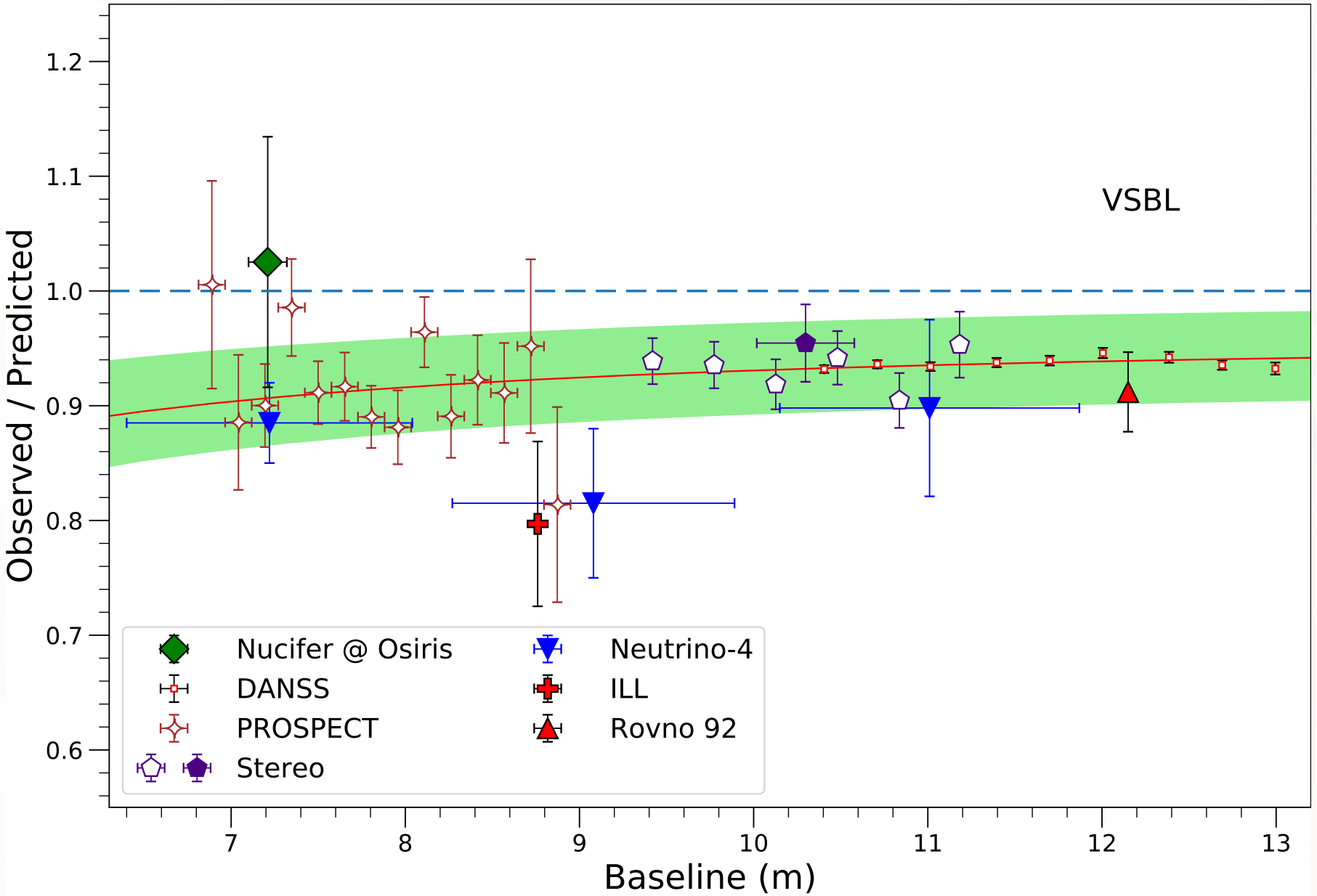

ISLV, Spectrum type = Fallot

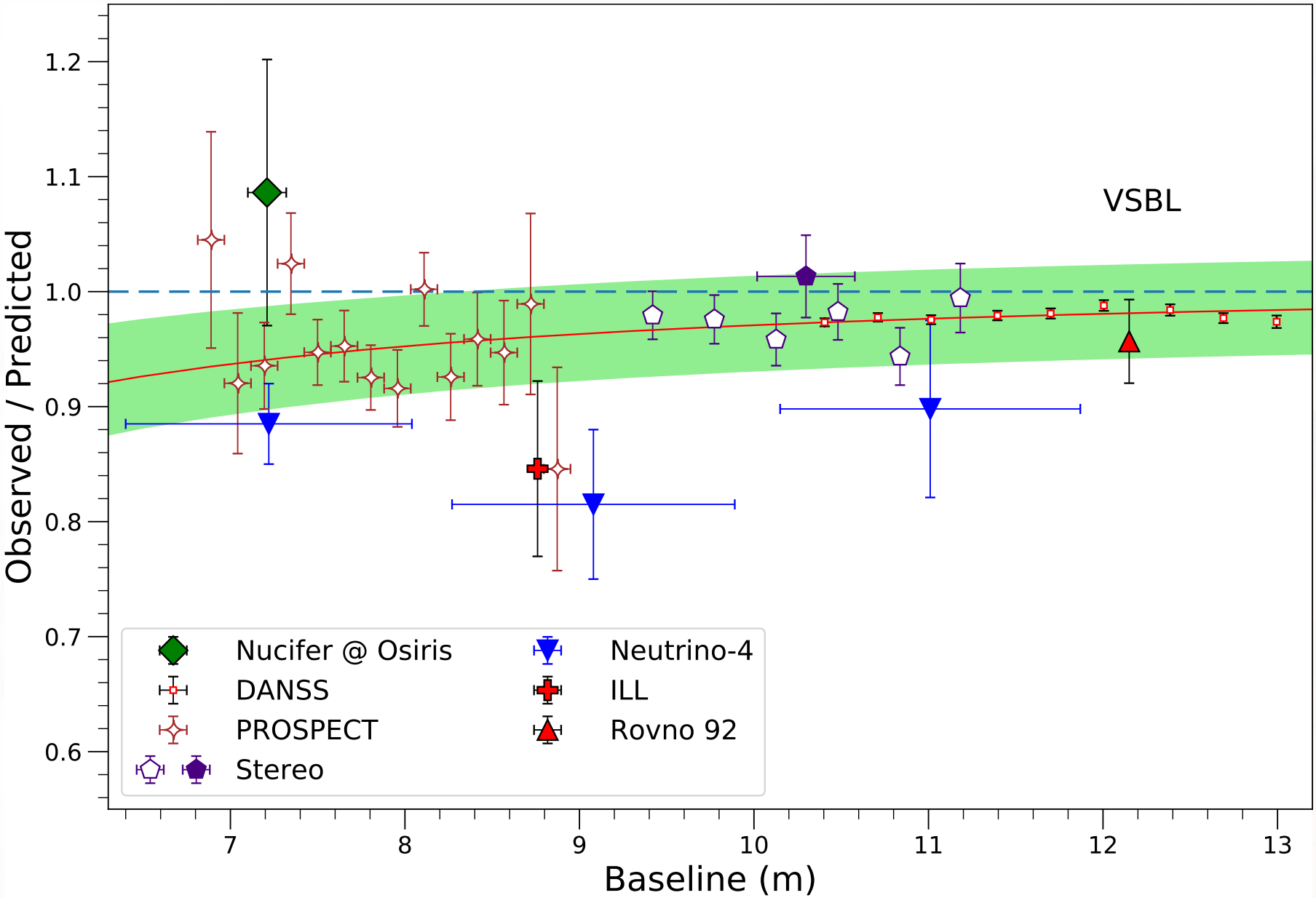

Marginalized 68% C.L. confidence contours

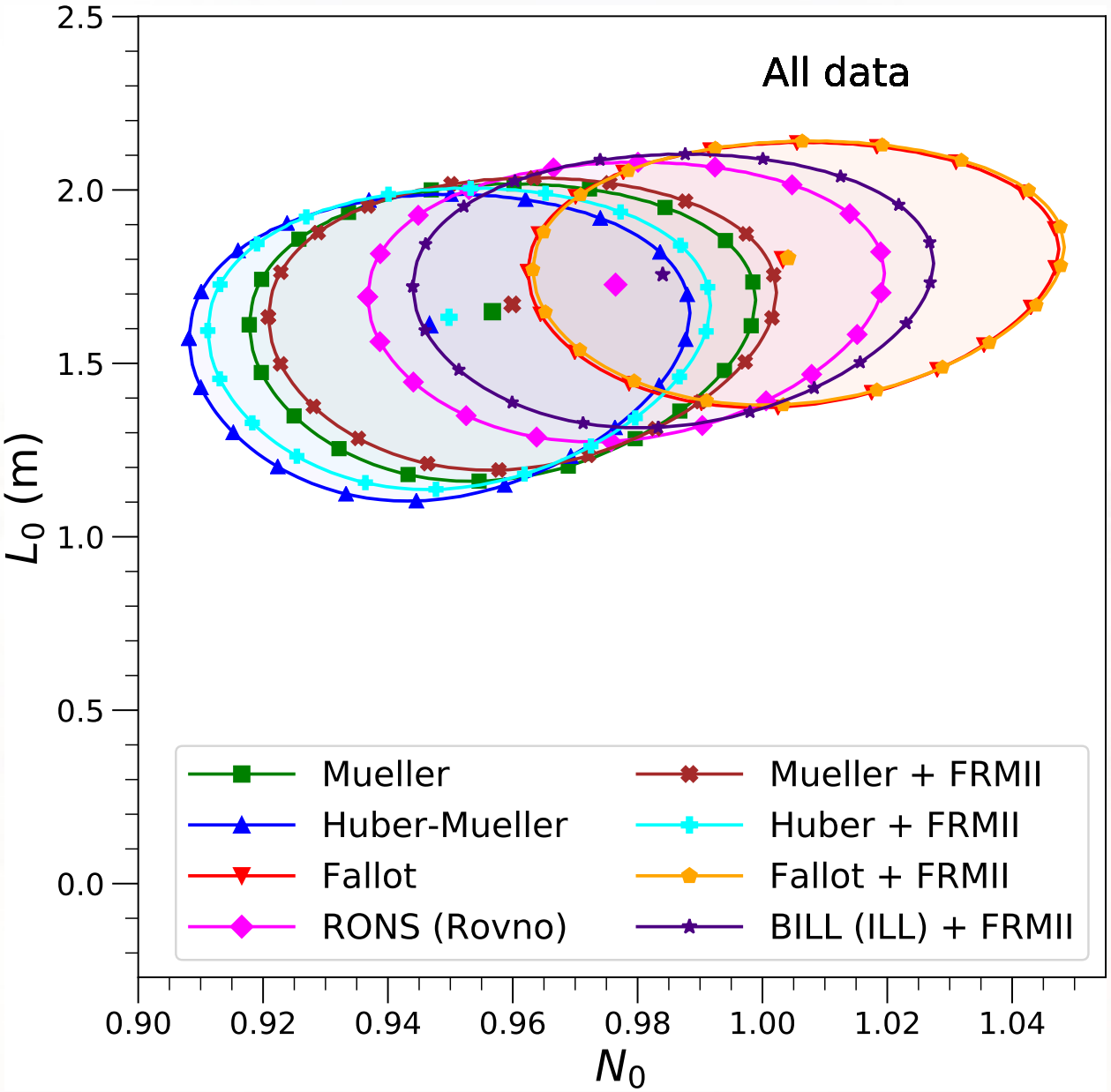

The 68% C.L. range:

$L_0 \approx (1.10 - 2.14)$ m

$\sigma_{\text{eff}} \approx (0.6 - 0.9)$ eV

From examination of the eight $\overline{\nu}_e$ spectrum models, we derived the following empirical correlations:

$$L_0 \approx 1.79 - 3.28\,(1 - N_0) \text{ m}$$

$$\frac{\chi^2}{\text{ndf}} \approx 0.86 - 2.56\,(1 - N_0)$$

Marginalized 68% C.L. confidence contours

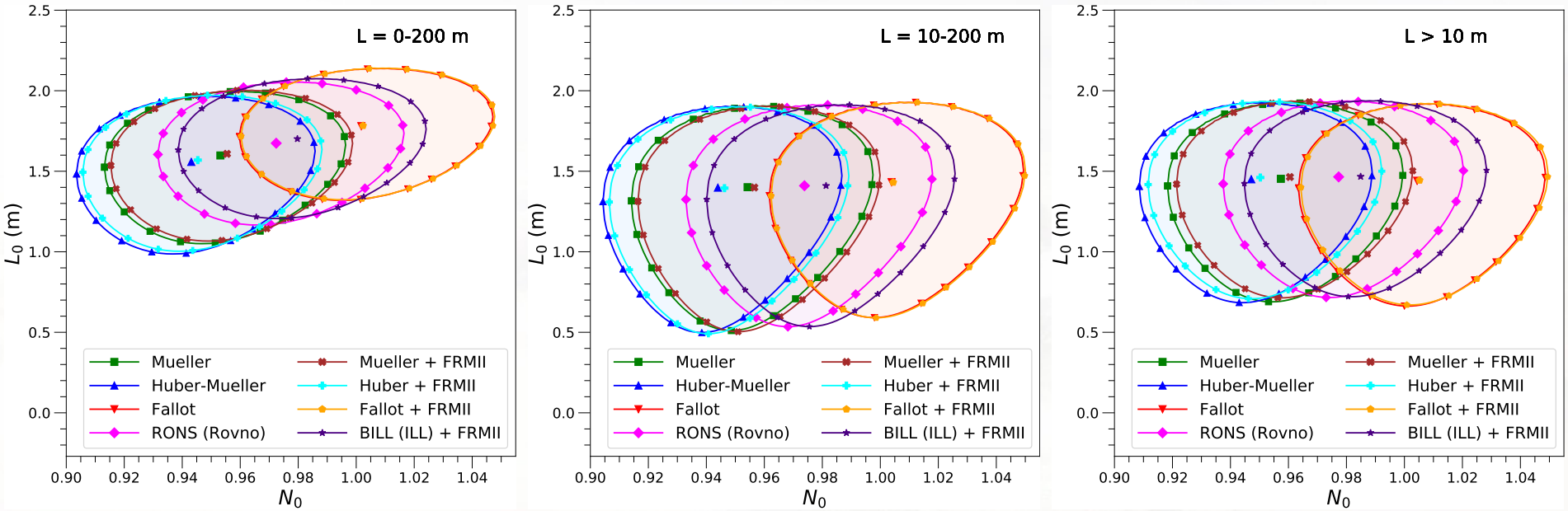

Confidence contours for the three data subsets and eight spectrum models show that the extracted value of L_0 is rather stable.

Relative measurements

Table ISL corrected ratios (K_{12}) of the IBD events measured at two distances (L_1, L_2) from reactor core by using movable or identical detectors

#	Experiment	Ref.	Comment	L_1 (m)	L_2 (m)	K_{12}
1	Gösgen (1984)	[13]	from inverse ratio	37.9	45.9	$0.99 \pm 0.03_{\text{stat.}} \pm 0.02_{\text{syst.}}$
2	Krasnoyarsk (1987)	[14]	from event number ratio	32.8	92.3	$0.984 \pm 0.168_{\text{stat.+syst.}}$
3	Krasnoyarsk (1990)	[15]	from event number ratio	57.0	57.6	$1.01 \pm 0.03_{\text{stat.+syst.}}$
4	Krasnoyarsk (1990)	[15]	from event number ratio	57.6	231.4	$0.86 \pm 0.22_{\text{stat.+syst.}}$
5	Krasnoyarsk (1990)	[15]	from event number ratio	57.0	231.4	$0.87 \pm 0.22_{\text{stat.+syst.}}$
6	Krasnoyarsk (1994)	[16]	from event number ratio	57.0	231.4	$0.86 \pm 0.15_{\text{stat.+syst.}}$
7	Rovno (1986)	[17]		18	25	$0.986 \pm 0.040_{\text{stat.}} \pm 0.029_{\text{syst.}}$
8	Rovno (1988)	[18]	from inverse ratio	18	25	$0.987 \pm 0.039_{\text{stat.+syst.}}$
9	Rovno (1991)	[19]	from cross section ratio	325.66	336.38	$0.993 \pm 0.042_{\text{stat.+syst.}}$
10	Rovno (1992)	[20]		12.15	18.34	$0.976 \pm 0.020_{\text{stat.}} \pm 0.015_{\text{syst.}}$
11	SRP (1996)	[21]	from event number ratio	18.18	23.82	$0.938 \pm 0.012_{\text{stat.}} \pm 0.017_{\text{syst.}}$
12	Bugey (1988)	[22]	from integrated spectra	13.63	18.30	$0.997 \pm 0.020_{\text{stat.}} \pm 0.021_{\text{syst.}}$
13	Bugey (1988)	[22]	from standard shielding data	13.63	18.30	$1.008 \pm 0.039_{\text{stat.}} \pm 0.021_{\text{syst.}}$
14	Bugey (1988)	[22]	from data with lowest threshold	13.63	18.30	$1.007 \pm 0.021_{\text{stat.}} \pm 0.021_{\text{syst.}}$
15	Bugey (1995)	[23]	from inverse spectrum ratio	15	40	$1.004 \pm 0.015_{\text{stat.}}$
16	Bugey (1995)	[23]	from inverse spectrum ratio	15	95	$0.997 \pm 0.146_{\text{stat.}}$

The ISLV expected ratio is $K_{12}^{\text{ISLV}} = 1 - L_0^2 x_{12}^2 + O\left(L_0^4/L_2^4\right)$, where $x_{12} = \sqrt{1/L_1^2 - 1/L_2^2}$.

Relative measurements

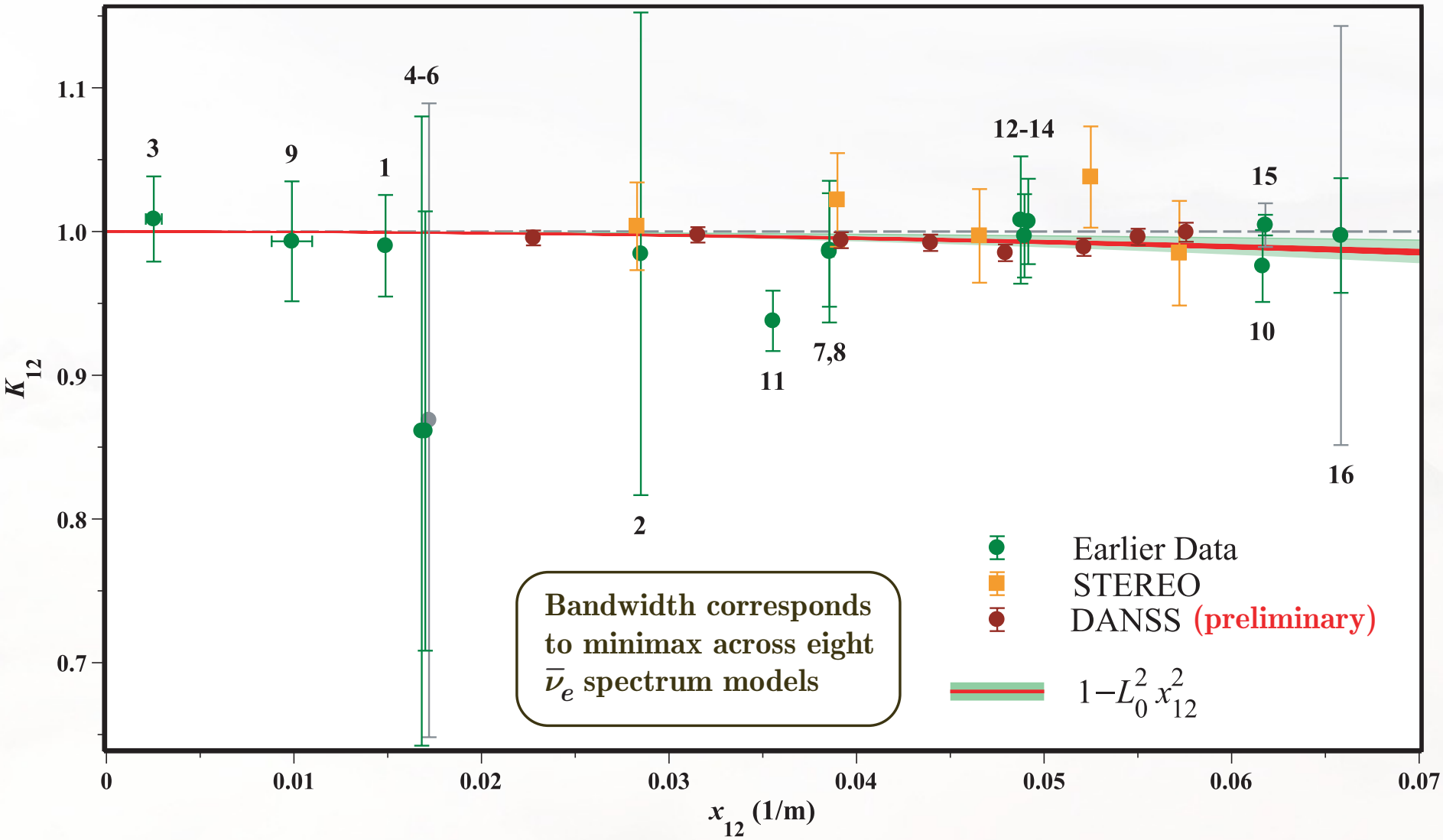

This dataset does not contradict the ISLV solution but provides no significant support to it (p-value = 1). However, the future potential of DANSS is clearly seen.

Gallium neutrino anomaly (GNA)

	GALLEX ($GaCl_3$:HCl) m(Ga)=30 t		SAGE (Ga metal) m(Ga)=13.1 t	
Source	^{51}Cr -1	^{51}Cr -2	^{51}Cr	^{37}Ar
Activity (MCi)	1.714	1.868	0.517	0.409
$R=\frac{\text{measured rate}}{\text{predicted rate}}$	0.953 ± 0.11	$0.812\,^{+0.10}_{-0.11}$	0.95 ± 0.12	$0.791\,^{+0.084}_{-0.078}$
$R_{combined}$	0.88 ± 0.08		0.86 ± 0.08	

The differences in activities and in target masses result in equal uncertainties of the experiments due to different sensitivities & dimensions of the sources.

The combined result of the four experiments: $R = 0.87 \pm 0.05$

The quality of fit to the average value: $\chi^2/dof = 1.9/3$, **GOF = 59%**

The ratios have been calculated with respect to the rate estimated using the best-fit values of the cross section of the detection process $\nu_e + {}^{71}Ga \rightarrow {}^{71}Ge + e^-$ calculated by Bahcall. Haxton's calculation decreases the ratios on about **13%**.

GNA: Ratios for different cross sections models

Detection of the Cr and Ar ν_es is achieved through the charged-current neutrino-nucleus scattering reaction

$$\nu_e + {}^{71}\mathrm{Ga}_{\text{ground state}} \rightarrow {}^{71}\mathrm{Ge}_{\text{lowest (4-5) excited states}} + e^- .$$

The corresponding cross sections are model dependent.[17]

Table Ratios of measured and expected ^{71}Ge event rates in the four radioactive source experiments calculated with several models of gallium cross sections for ^{51}Cr and ^{37}Ar neutrinos.

#	Model by	Ref.	GALLEX-1	GALLEX-2	SAGE-1	SAGE-2
1	Bahcall	[25]	0.95 ± 0.11	0.81 ± 0.11	0.95 ± 0.12	0.79 ± 0.08
2	Haxton	[24, 26]	0.86 ± 0.13	0.74 ± 0.12	0.86 ± 0.14	0.72 ± 0.10
3	Frekers *et al.*	[27]	0.93 ± 0.11	0.79 ± 0.11	0.93 ± 0.12	0.77 ± 0.08
4	JUN45	[24, 28]	0.97 ± 0.11	0.83 ± 0.11	0.97 ± 0.12	0.81 ± 0.08
5	Barinov *et al.*	[29]	0.93 ± 0.11	0.80 ± 0.11	0.93 ± 0.12	$0.77^{+0.09}_{-0.08}$

[17] See, e.g., J. Kostensalo *et al. Phys. Lett. B* **795** (2019) 542. arXiv: 1906.10980 [nucl-th].

GNA: Is this related to ISLV?

- **If** the ISLV mechanism really works for reactor's $\overline{\nu}_e$s, it **must** work also for the Cr and Ar ν_es.
- From the extended GS theorem it follows that

$$L_0 \sim \langle E_\nu/\sigma^2_{\rm eff}\rangle \sim \overline{E}_\nu/\overline{\sigma}^2_{\rm eff}.$$

- For a **very rough** estimations, let's speculate that $\sigma_{\rm eff}$ is the same in the reactor and gallium experiments.
- Then, considering that $\overline{E}_\nu^{\rm reactor} = (4.2 - 4.4)$ MeV and using the data on decay modes of the isotopes (see table), we can estimate the lengths:

$$L_0^{\text{Cr-51}} \sim L_0^{\rm reactor}\,\frac{\overline{E}_\nu^{\text{Cr-51}}}{\overline{E}_\nu^{\rm reactor}} \approx 29\ {\rm cm}, \quad L_0^{\text{Ar-37}} \sim L_0^{\rm reactor}\,\frac{\overline{E}_\nu^{\text{Ar-37}}}{\overline{E}_\nu^{\rm reactor}} \approx 32\ {\rm cm}.$$

Isotope	E_ν (keV)	f (%)	$\sigma(E_\nu)\,(10^{-46}\,{\rm cm}^2)$	E_ν (keV)	f (%)	$\sigma(E_\nu)\,(10^{-46}\,{\rm cm}^2)$
^{51}Cr	752	8.49	63.22 ± 1.40	432	0.93	27.14 ± 0.52
	747	81.63	62.58 ± 1.39	427	8.95	26.72 ± 0.51
^{37}Ar	813	9.80	71.63 ± 1.62	811	90.20	71.35 ± 1.61

GNA: Comparison with data

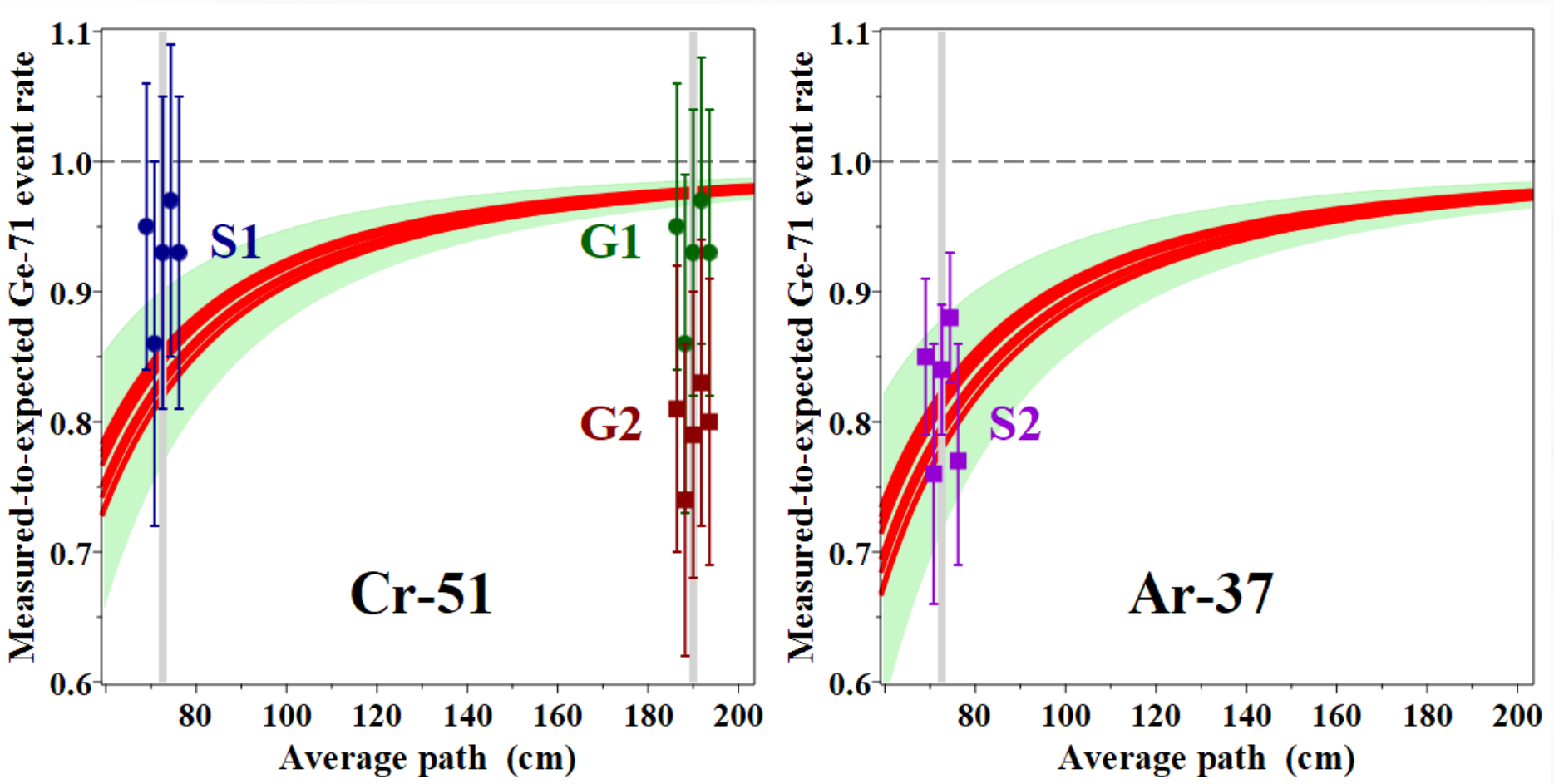

- Eight curves are calculated with $L_0^{\text{Cr-51}}$ and $L_0^{\text{Ar-37}}$ obtained from the best-fit L_0^{reactor} for eight $\overline{\nu}_e$ spectrum models; bandwidths correspond to the 1σ minimax over all these models.
- For visual clarity, the points (re)evaluated from the original data with 5 cross-section models are left/right shifted from corresponding average paths, indicated by narrow vertical strips.

Summary

- The QFT approach predicts that the classical inverse-square law could be broken at short (macroscopic) distances.
- Current reactor data hint that the ISLV is already seen.
- Taking into account essential uncertainty in the $\overline{\nu}_e$ spectrum calculations, the RAA can be explained without sterile νs, but not excluding the latter.
- With less certainty, the same is true for the gallium data. Experiments with small intense $\nu/\overline{\nu}$ sources and sectioned detector(s) are required.
- Well, what if the new data (say from DANSS) closes our explanation? It'll be a pity, but it'll not mean a confutation of the QFT approach or extended GS theorem. Rather, it'll only be an indication that σ_{eff} is above the sensitivity threshold.
- Studying the spectral reactor measurements will be needed when (and if) the new data will more definitely confirm the ISLV.

We are grateful to Igor Alekseev, Mikhail Danilov, Anatael Cabrera, Muriel Fallot, Maxim Gonchar, Alain Letourneau, Beda Roskovec, and Zhe Wang for providing us with their results.
We thank Igor Kakorin, Konstantin Kuzmin, and Dmitry Naumov for helpful comments, conversations, and suggestions.

Thanks for attention!

[1] D. V. Naumov, V. A. Naumov, and D. S. Shkirmanov. *Phys. Part. Nucl.* **48**.1 (2017) 12. arXiv: 1507.04573 [hep-ph].

[2] D. V. Naumov, V. A. Naumov, and D. S. Shkirmanov. *Phys. Part. Nucl.* **48**.6 (2017) 1007.

[3] V. A. Naumov and D. S. Shkirmanov. *Eur. Phys. J. C* **73** (2013) 2627. arXiv: 1309.1011 [hep-ph].

[4] S. E. Korenblit and D. V. Taychenachev. *Mod. Phys. Lett.* **A 30** (2015) 1550074. arXiv: 1401.4031 [math-ph].

[5] J. M. Berryman and P. Huber. arXiv: 2005.01756 [hep-ph].

[6] J. Kopp *et al. JHEP* **05** (2013) 050. arXiv: 1303.3011v2 [hep-ph].

[7] A. C. Hayes *et al. Phys. Rev. Lett.* **112** (2014) 202501. arXiv: 1309.4146 [nucl-th].

[8] D. V. Naumov and V. A. Naumov. *J. Phys.* **G 37** (2010) 105014. arXiv: 1008.0306v2 [hep-ph].

[9] G. Mention *et al. Phys. Rev.* **D 83** (2011) 073006. arXiv: 1101.2755 [hep-ex].

[10] C. Zhang, X. Qian, and P. Vogel. *Phys. Rev.* **D 87** (2013) 073018. arXiv: 1303.0900 [nucl-ex].

[11] Th A. Mueller *et al. Phys. Rev.* **C 83** (2011) 054615. arXiv: 1101.2663 [hep-ex].

[12] A. N. Ivanov *et al. Phys. Rev.* **C 88** (2013) 055501. arXiv: 1306.1995v2 [hep-ph].

[13] K. Gabathuler *et al. Phys. Lett.* **B 138** (1984) 449.

[14] G. S. Vidyakin *et al. Zh. Eksp. Teor. Fiz.* **93** (1987) 424.

[15] G. S. Vidyakin *et al. Zh. Eksp. Teor. Fiz.* **98** (1990) 764.

[16] G. S. Vidyakin *et al. Pisma Zh. Eksp. Teor. Fiz.* **59** (1994) 364.

[17] A. I. Afonin *et al. Pisma Zh. Eksp. Teor. Fiz.* **44** (1986) 111.

[18] A. I. Afonin *et al. Zh. Eksp. Teor. Fiz.* **94** (1988) 1.

[19] A. A. Kuvshinnikov *et al. Pisma Zh. Eksp. Teor. Fiz.* **54** (1991) 259.

[20] S. N. Ketov *et al. Pisma Zh. Eksp. Teor. Fiz.* **55** (1992) 544.

[21] Z. D. Greenwood *et al. Phys. Rev.* **D 53** (1996) 6054.

[22] Hervé De Kerret. *Proceedings of the 23rd Rencontre de Moreond "Fifth force, neutrino physics" (Neutrinos and Exotic Phenomena in Particle Physics and in Astrophysics Session), Les Arcs, Savoie, France, January 23–30, 1988*. Ed. by O. Fackler and J. Tran Thanh Van. Editions Frontières, Gif-sur-Yvette, France, 1988, pp. 125–131.

[23] B. Achkar *et al. Nucl. Phys.* **B 434** (1995) 503.

[24] J. Kostensalo *et al. Phys. Lett. B* **795** (2019) 542. arXiv: 1906.10980 [nucl-th].

[25] J. N. Bahcall. *Phys. Rev. C* **56** (1997) 3391. arXiv: hep-ph/9710491.

[26] W. C. Haxton. *Phys. Lett. B* **431** (1998) 110. arXiv: nucl-th/9804011.

[27] D. Frekers *et al. Phys. Lett. B* **706** (2011) 134.

[28] M. Honma *et al. Phys. Rev. C* **80** (2009) 064323.

[29] V. Barinov *et al. Phys. Rev. D* **97**.7 (2018) 073001. arXiv: 1710.06326 [hep-ph].

[30] L. A. Khalfin. *Zh. Eksp. Teor. Fiz.* **33** (1957) 1371.

[31] C. Bernardini, L. Maiani, and M. Testa. *Phys. Rev. Lett.* **71** (1993) 2687.

[32] S. Pascazio. *Open Syst. & Inf. Dyn.* **21** (2014) 1440007. arXiv: 1311.6645 [quant-ph].

[33] A. Gando *et al.* arXiv: 1312.0896 [physics.ins-det].

[34] K. N. Abazajian *et al.* arXiv: 1204.5379 [hep-ph].

[35] P.A.R. Ade *et al.* arXiv: 1303.5076 [astro-ph.CO].

[36] F. Reines, H. W. Sobel, and E. Pasierb. *Phys. Rev. Lett.* **45** (1980) 1307.

[37] M. Fallot *et al. Phys. Rev. Lett.* **109** (2012) 202504. arXiv: 1208.3877 [nucl-ex].

[38] V. V. Sinev. *Yad. Fiz.* **76** (2013) 578. arXiv: 1207.6956 [nucl-ex].

BACKUP

Non-exponential decay & Zeno paradox

Survival probability of an unstable QM state at **short** times is[18]

$$P_{\text{surv}} = \left|\left\langle e^{-i\mathbf{H}t}\right\rangle\right|^2 = 1 + \left(\langle\mathbf{H}\rangle^2 - \langle\mathbf{H}^2\rangle\right) t^2 + \ldots = 1 - \sigma_E^2 t^2 + \ldots, \qquad (9)$$

where σ_E^2 is the energy dispersion. So the decay probability, P_{dec}, vanishes as t^2, $t \to 0$, whereas the standard decay law says:

$$P_{\text{dec}} = 1 - e^{-t/\tau} = t/\tau + \ldots$$

Note that τ (and thus the "short" time, $t \ll \tau$) can actually be huge (say, $t \sim 10^{33}$ years).

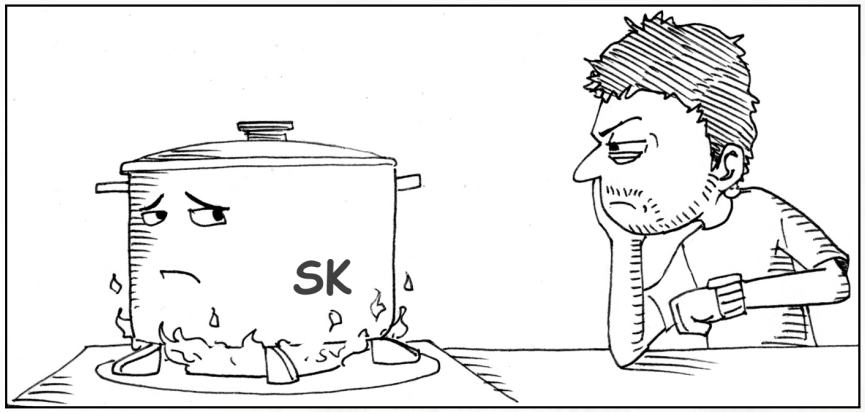

Watched quantum pots never boil.

Behavior (9) in particular leads to the so-called quantum Zeno paradox:

The decay probability being negligible at short times, a quantum system observed frequently after formation will never decay.

The parallel: finite-time evolution $\longleftrightarrow$ finite-distance propagation

[18] L. A. Khalfin. *Zh. Eksp. Teor. Fiz.* **33** (1957) 1371; for a more contemporary discussion, see C. Bernardini, L. Maiani, and M. Testa. *Phys. Rev. Lett.* **71** (1993) 2687 and references therein.

Non-exponential decay & Zeno paradox

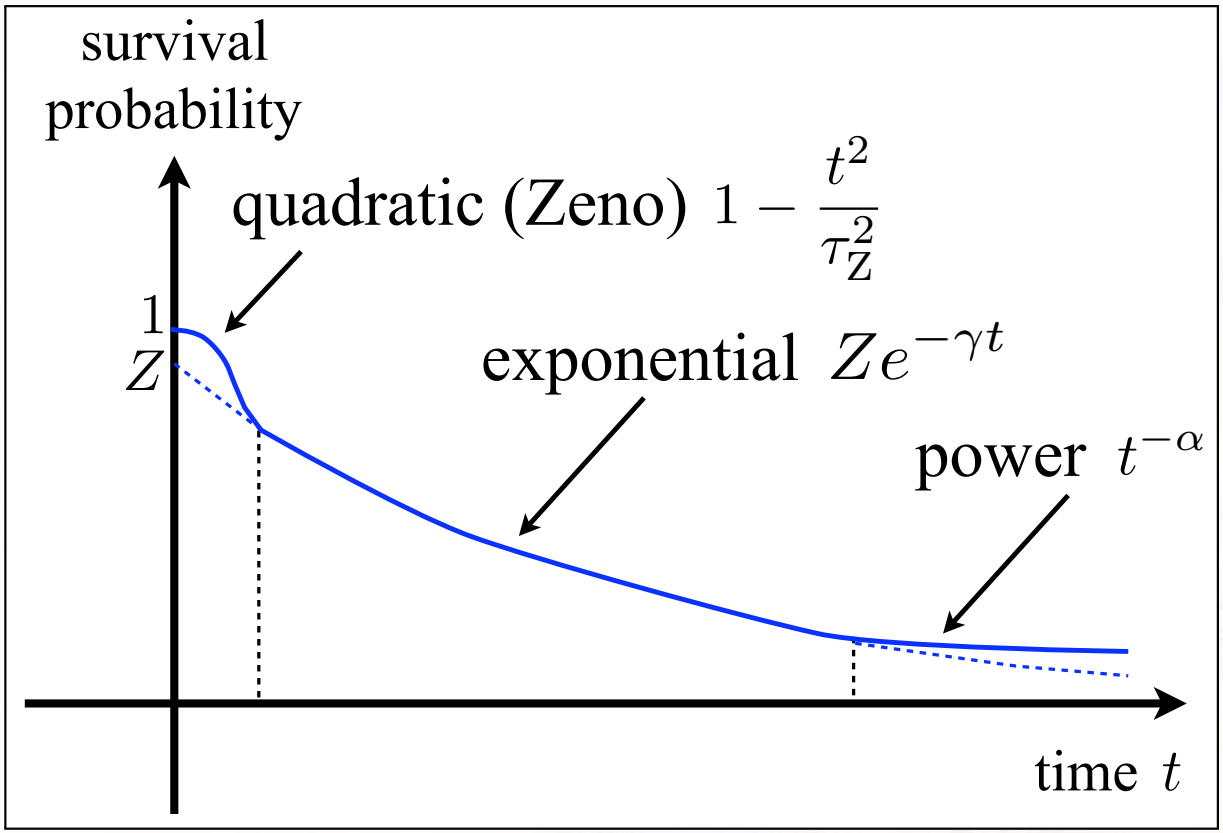

Survival probability of a decaying quantum system. The initial Zeno region is followed by an exponential decay and finally superseded by a power law. The extrapolation of the exponential law back to $t = 0$ yields a value Z that is in general $\neq 1$.[19]

[19] Borrowed from S. Pascazio. *Open Syst. & Inf. Dyn.* **21** (2014) 1440007. arXiv: 1311.6645 [quant-ph].

Reaction $\pi \oplus n \rightarrow \mu \oplus \tau p$

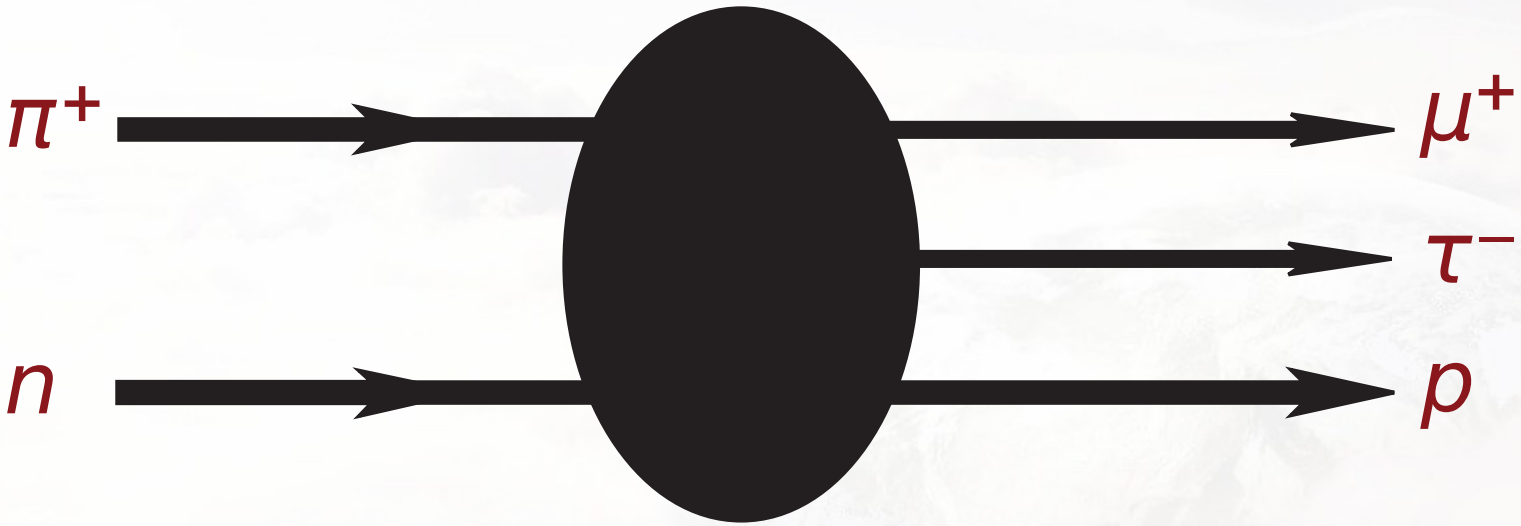

The rare reactions

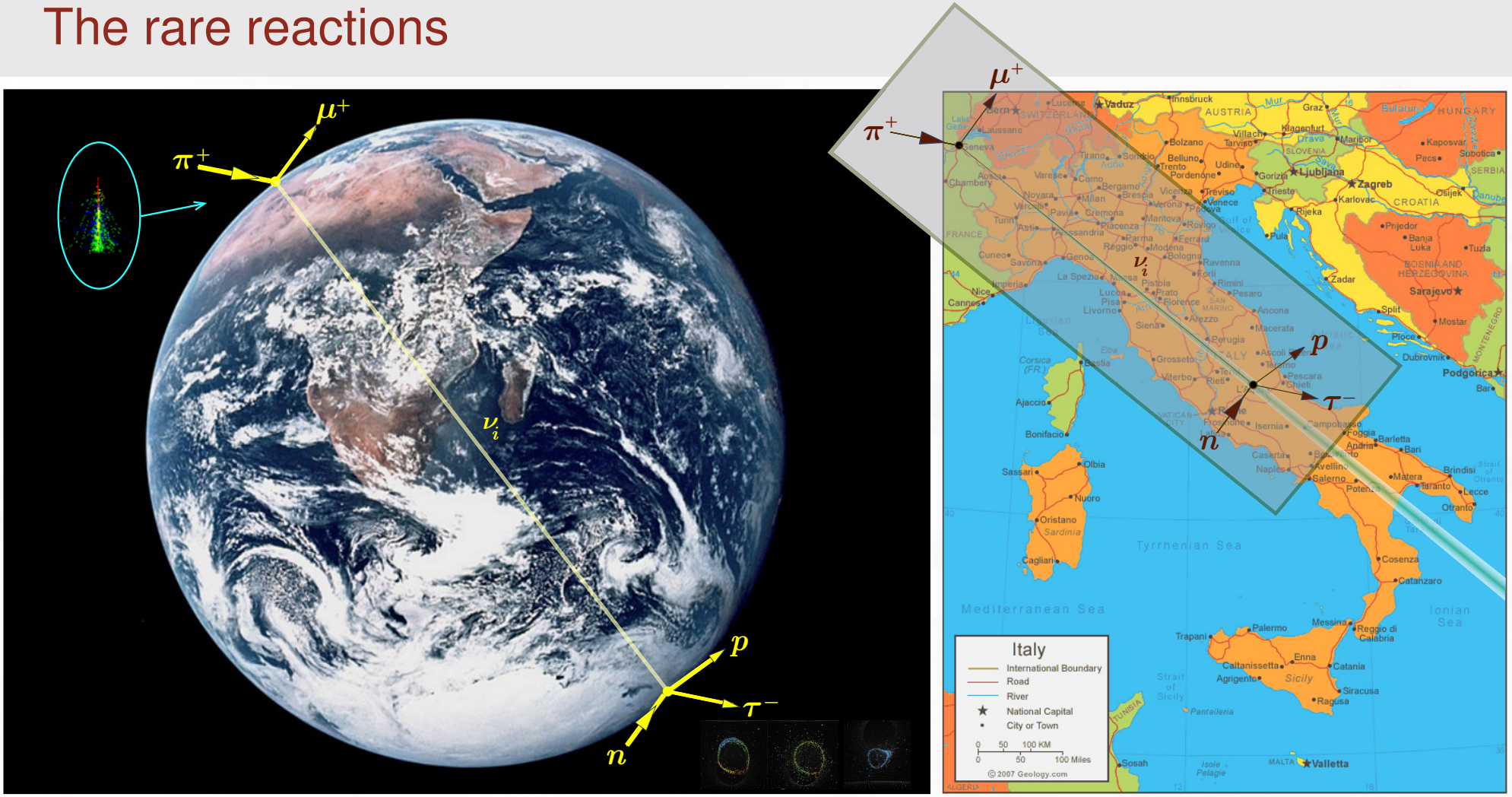

The rare reactions $\pi^+ \oplus n \to \mu^+ \oplus \tau^- p + \ldots$ were indirectly detected in the underground experiments Kamiokande, IMB & Super-Kamiokande with atmospheric neutrinos. In 2010, OPERA experiment (LNGS) with the CNGS ν_μ beam announced the direct observation of a τ^- candidate event; five candidates were recorded during the next several years.

QFT approach

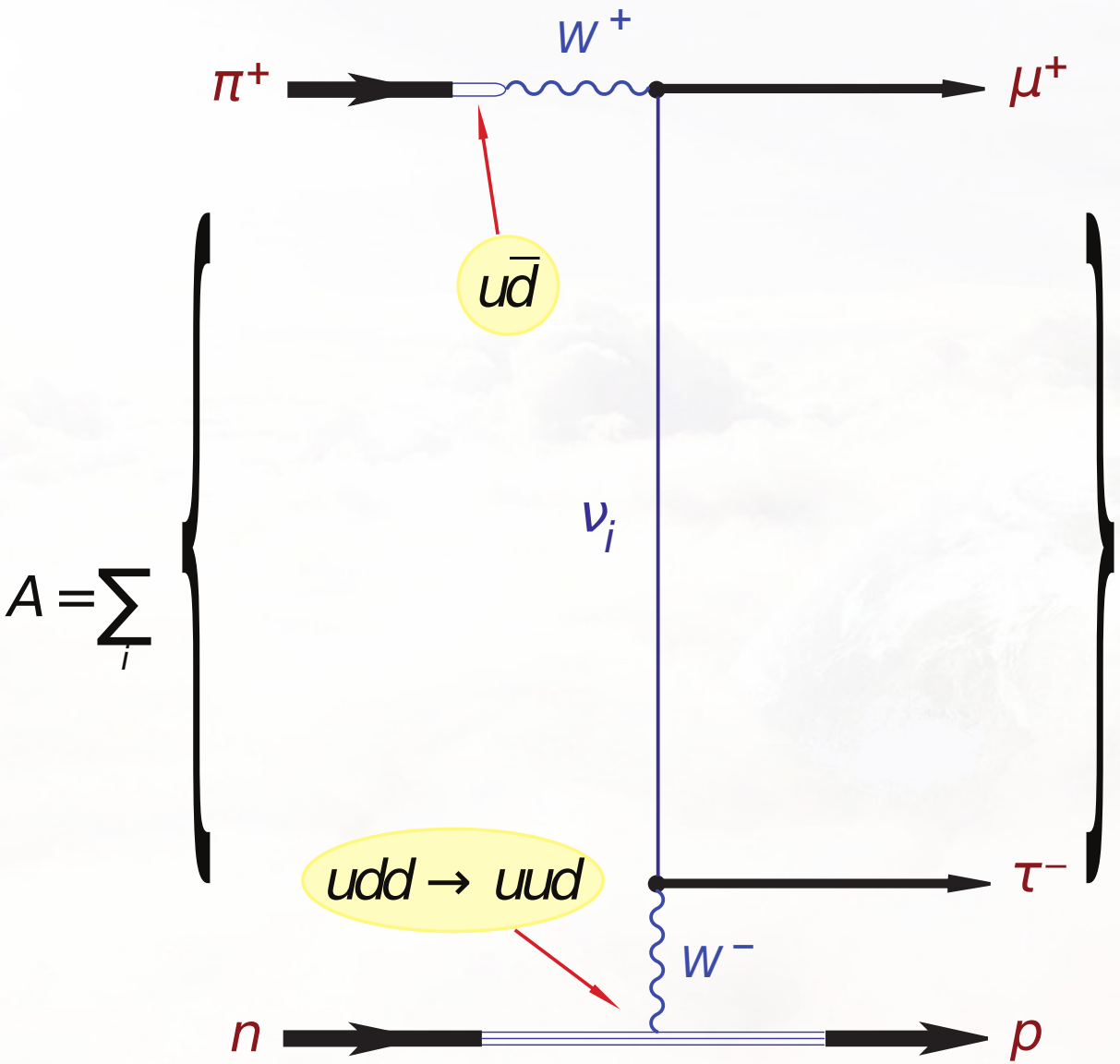

QFT approach

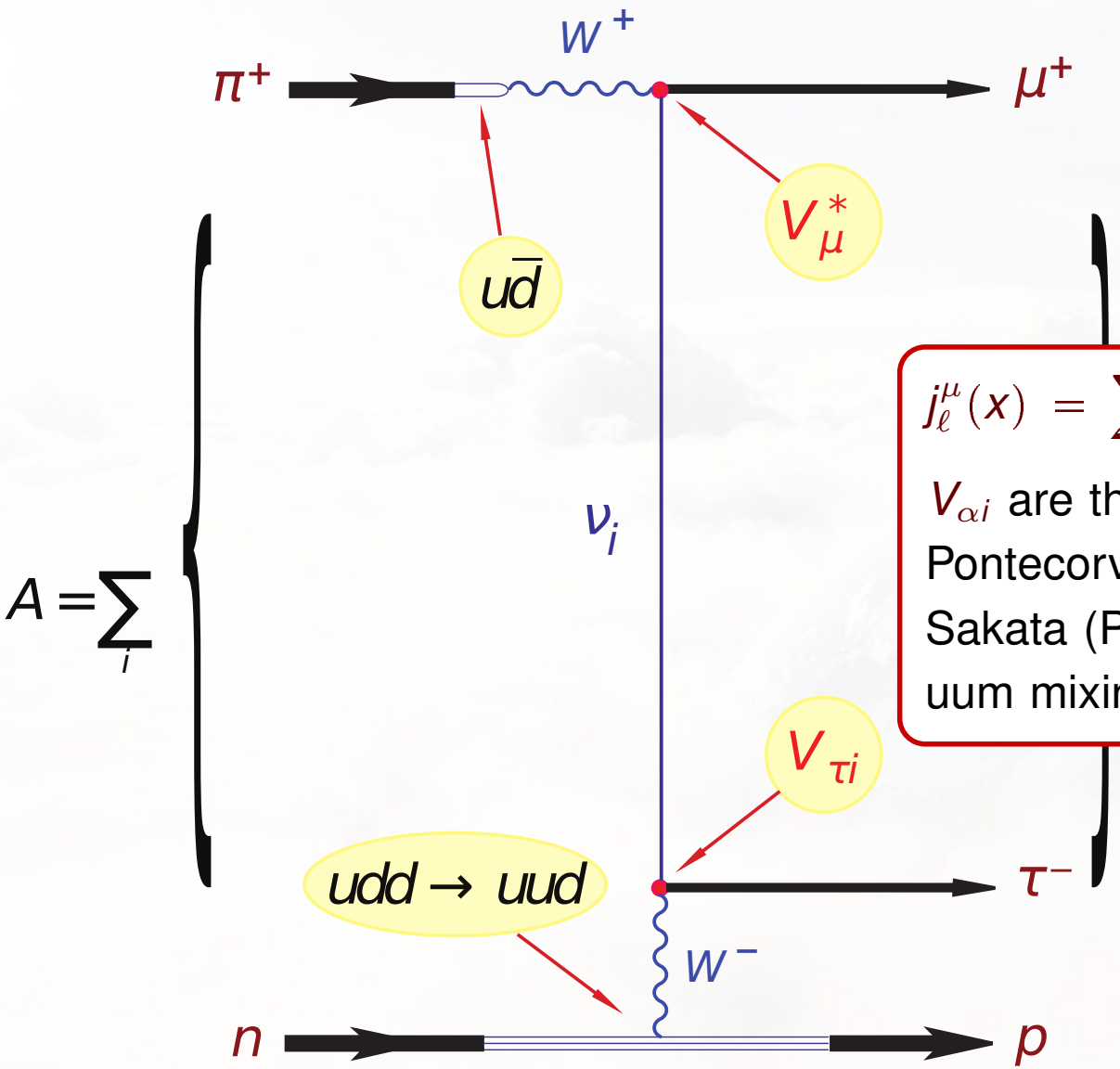

$$j^\mu_\ell(x) = \sum_{\alpha i} V^*_{\alpha i}\, \overline{\nu}_i(x) O^\mu \ell_\alpha(x)$$

$V_{\alpha i}$ are the elements of the Pontecorvo-Maki-Nakagawa-Sakata (PMNS) neutrino vacuum mixing matrix **V**.

QFT approach

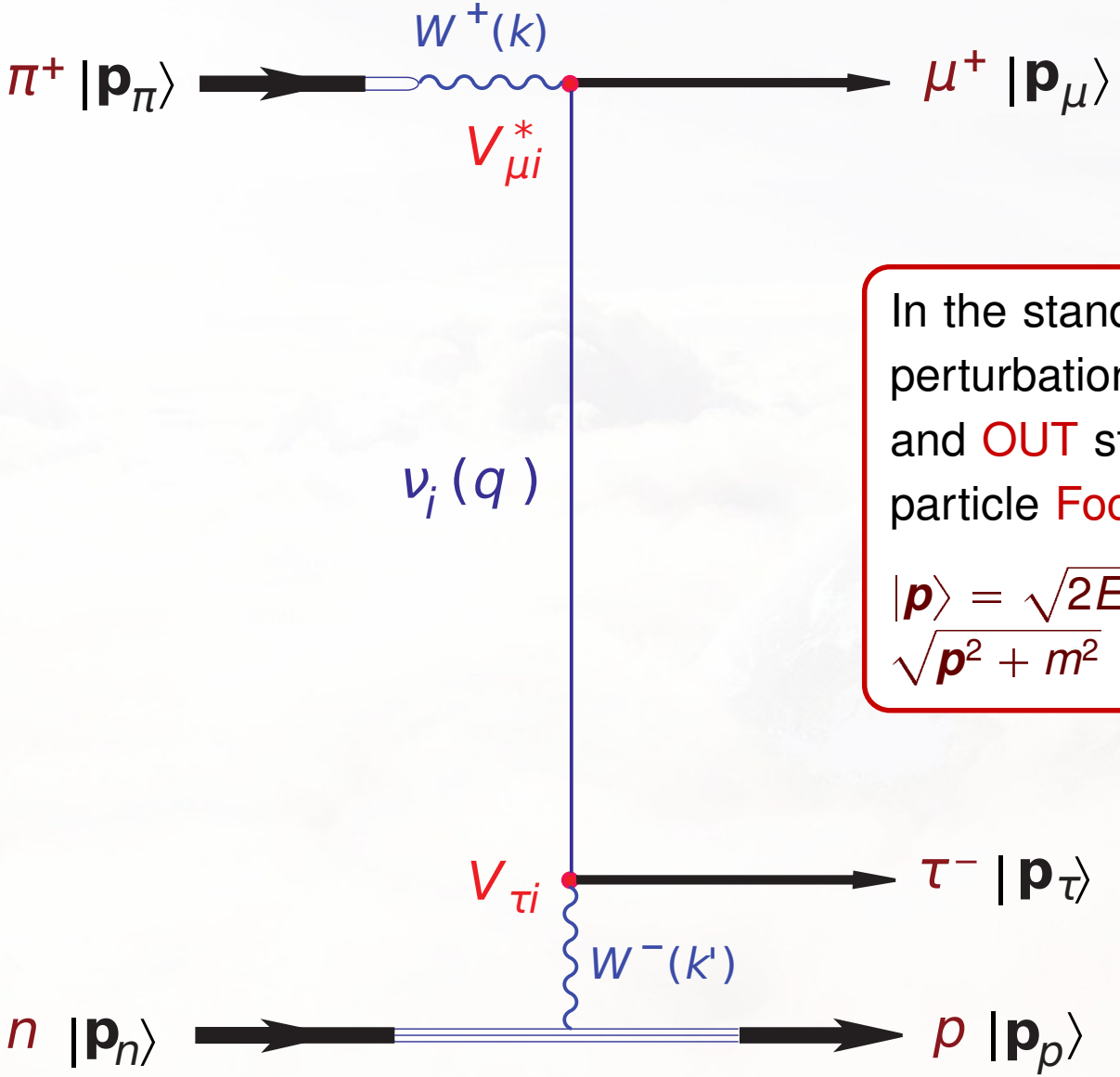

In the standard S matrix perturbation theory the IN and OUT states are one-particle Fock states:

$$|\boldsymbol{p}\rangle = \sqrt{2E_{\boldsymbol{p}}}a^+(\boldsymbol{p})|0\rangle \; E_{\boldsymbol{p}} = \sqrt{\boldsymbol{p}^2 + m^2}$$

QFT approach

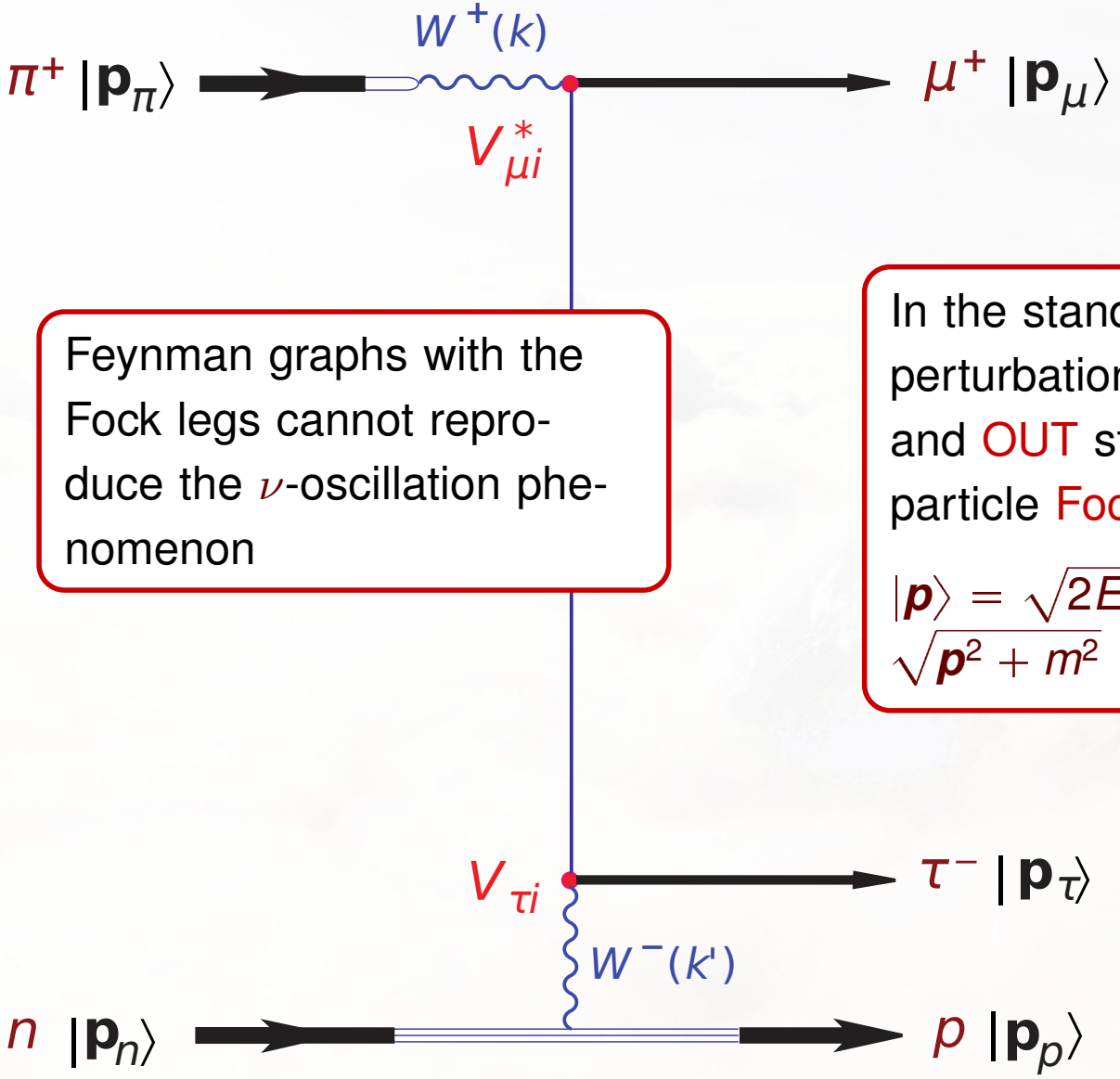

Feynman graphs with the Fock legs cannot reproduce the ν-oscillation phenomenon

In the standard S matrix perturbation theory the IN and OUT states are one-particle Fock states:

$$|\boldsymbol{p}\rangle = \sqrt{2E_{\boldsymbol{p}}}a^+(\boldsymbol{p})|0\rangle \; E_{\boldsymbol{p}} = \sqrt{\boldsymbol{p}^2 + m^2}$$

QFT approach

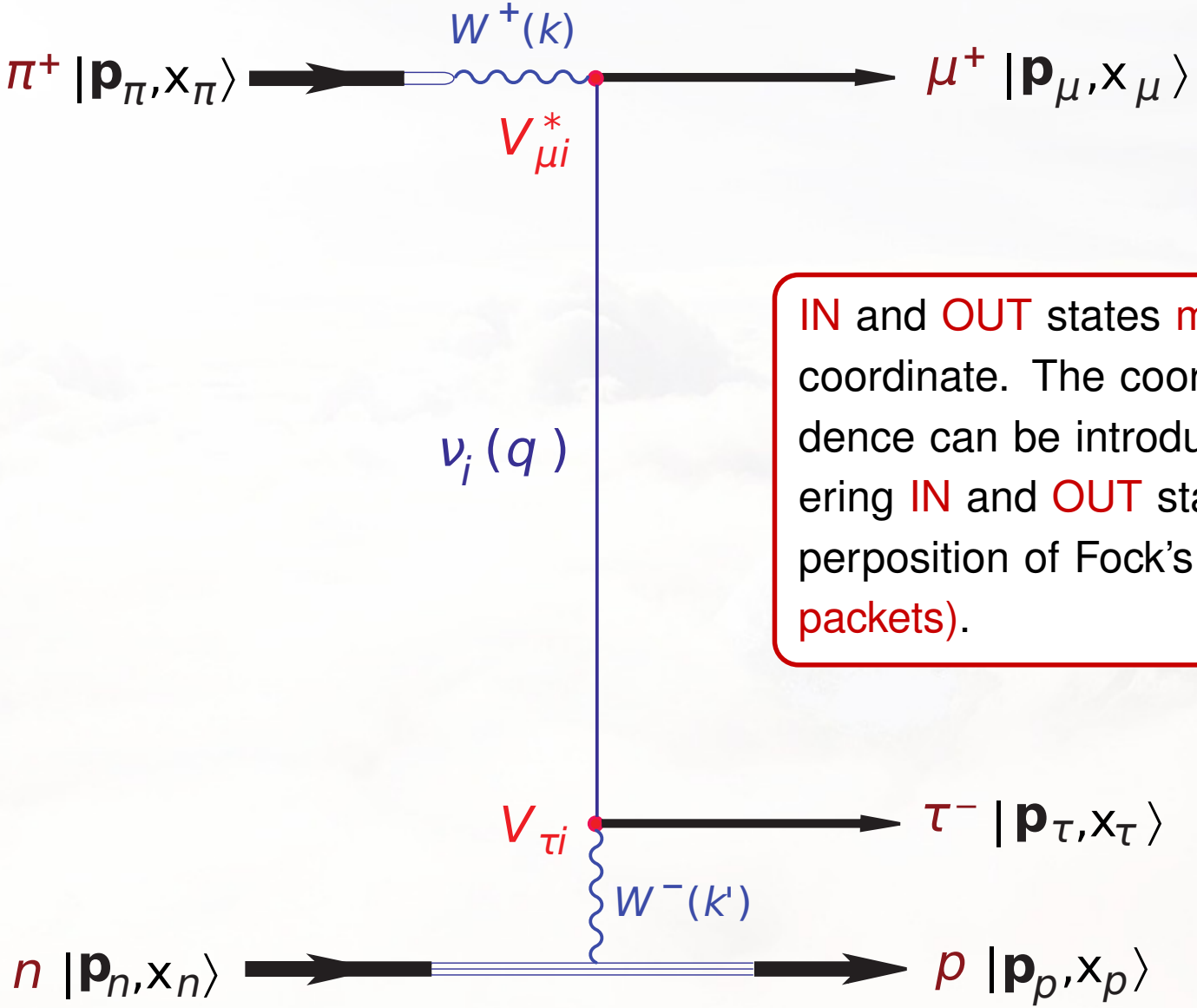

IN and OUT states must have a coordinate. The coordinate dependence can be introduced by considering IN and OUT states as a superposition of Fock's states (wave packets).

QFT approach

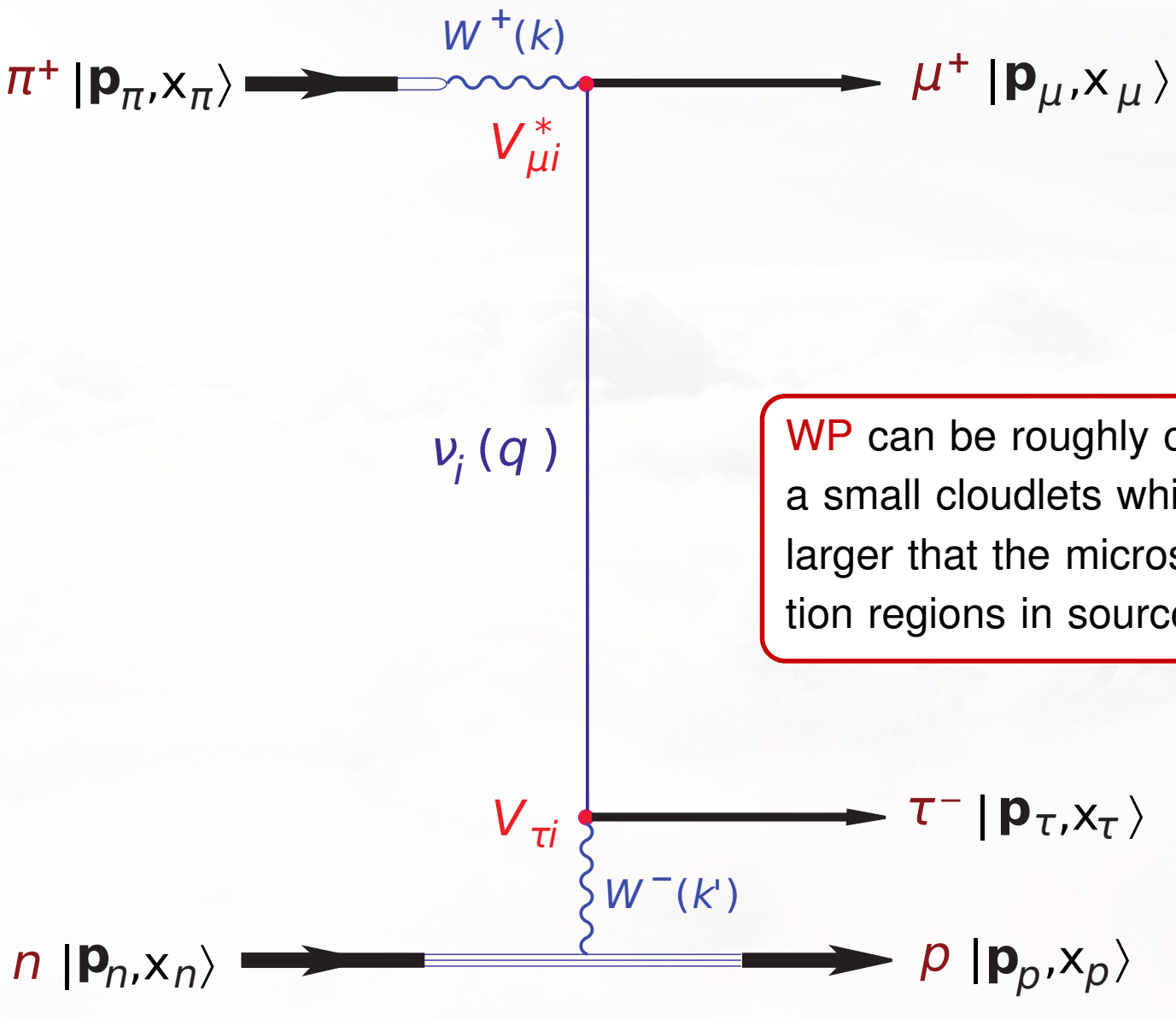

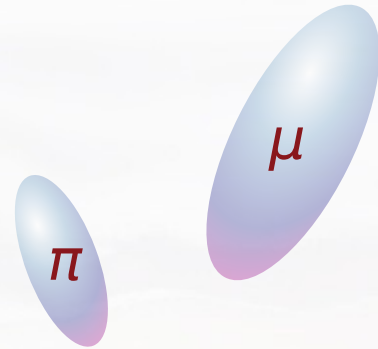

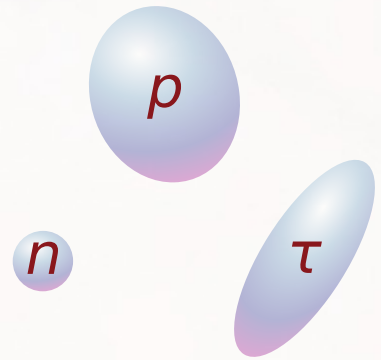

WP can be roughly considered as a small cloudlets which are much larger that the microscopic interaction regions in source and detector.

QFT approach

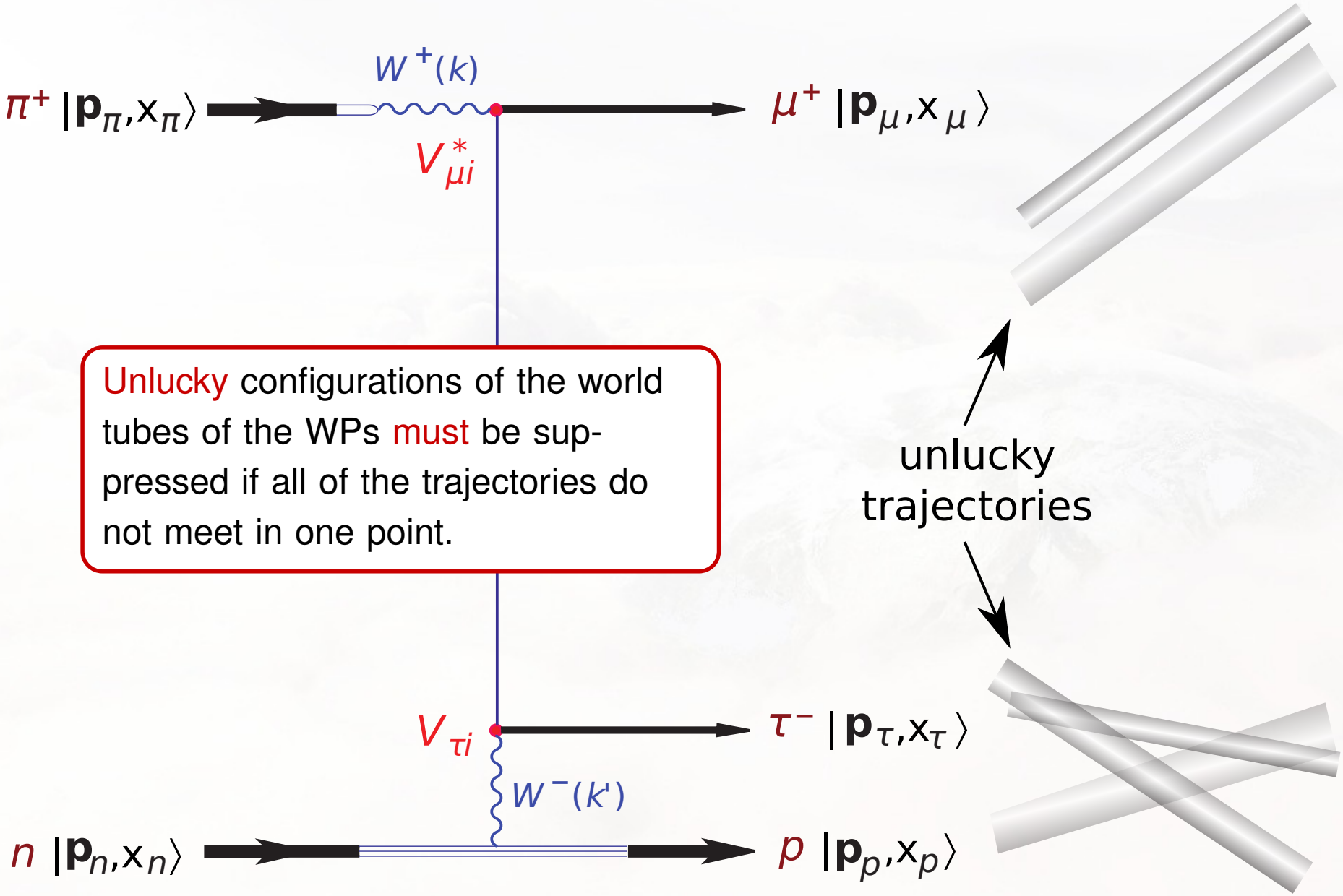

QFT approach

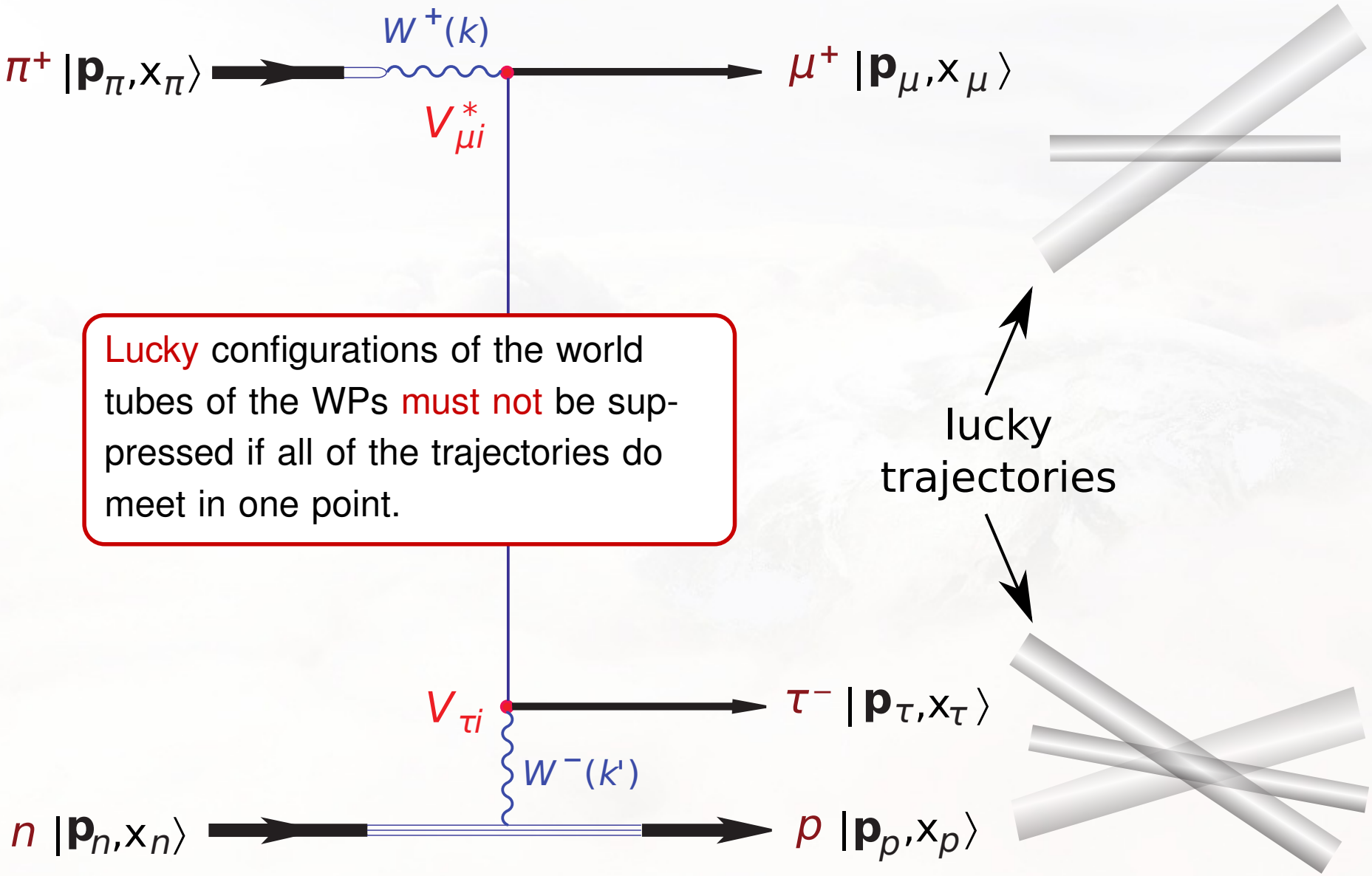

Coordinate dependence of states

- Within the framework of the plane-wave formalism of Quantum Field Theory the particles states are defined as Fock's states:

$$|\boldsymbol{k}, s\rangle = \sqrt{2E_{\boldsymbol{k}}}\, a^{\dagger}_{\boldsymbol{k}s}|0\rangle. \tag{10}$$

- The Fock states have no information about the coordinate of the particle.
- ★ To introduce dependence on the coordinate one needs to build a wave packet that is superposition of Fock's states:

$$|\boldsymbol{p}, s, x\rangle = \int \frac{d\boldsymbol{k}\, \phi(\boldsymbol{k}, \boldsymbol{p}) e^{i(k-p)x}}{(2\pi)^3 2E_{\boldsymbol{k}}} |\boldsymbol{k}, s\rangle. \tag{11}$$

Amplitude

To calculate amplitude of some process $\alpha \to \beta$ one should construct the matrix element that is defined by the same expression as in ordinary Quantum Field Theory:

$$\langle \mathbf{out}|\mathbb{S}|\mathbf{in}\rangle \left(\langle \mathbf{in}|\mathbf{in}\rangle\langle \mathbf{out}|\mathbf{out}\rangle\right)^{-1/2} \stackrel{\text{def}}{=} \mathcal{A}_{\beta\alpha}.$$

The difference from standard, plane-wave QFT is that now IN and OUT states are wave packets, not Fock's states.

CRGP model amplitude properties

- Based on the CRGP model the amplitude of process $I_s \oplus I_d \rightarrow F_s \oplus F_d$ can be calculated.
- The amplitude produces standard oscillating factor responsible for the neutrino oscillations.
- The amplitude is suppressed if particles trajectories do not meet in one point either in source or detector.
- The amplitude is approximately proportional to $1/L$, as a result the neutrino event rate is approximately proportional to $1/L^2$ (the inverse-square law).

Macroscopic Feynman diagrams

- Our approach operates with the macroscopic Feynman diagrams.
- Here X_d and X_d denote the regions where the intermediate neutrino was born and detected, respectively. These regions are macroscopically separated in the space-time,
- $I_{s,d}$ denote initial particles in the source and detector vertices, respectively; $F_{s,d}$, $F'_{s,d}$ denote the sets of final particles (the notation is clear from the picture).

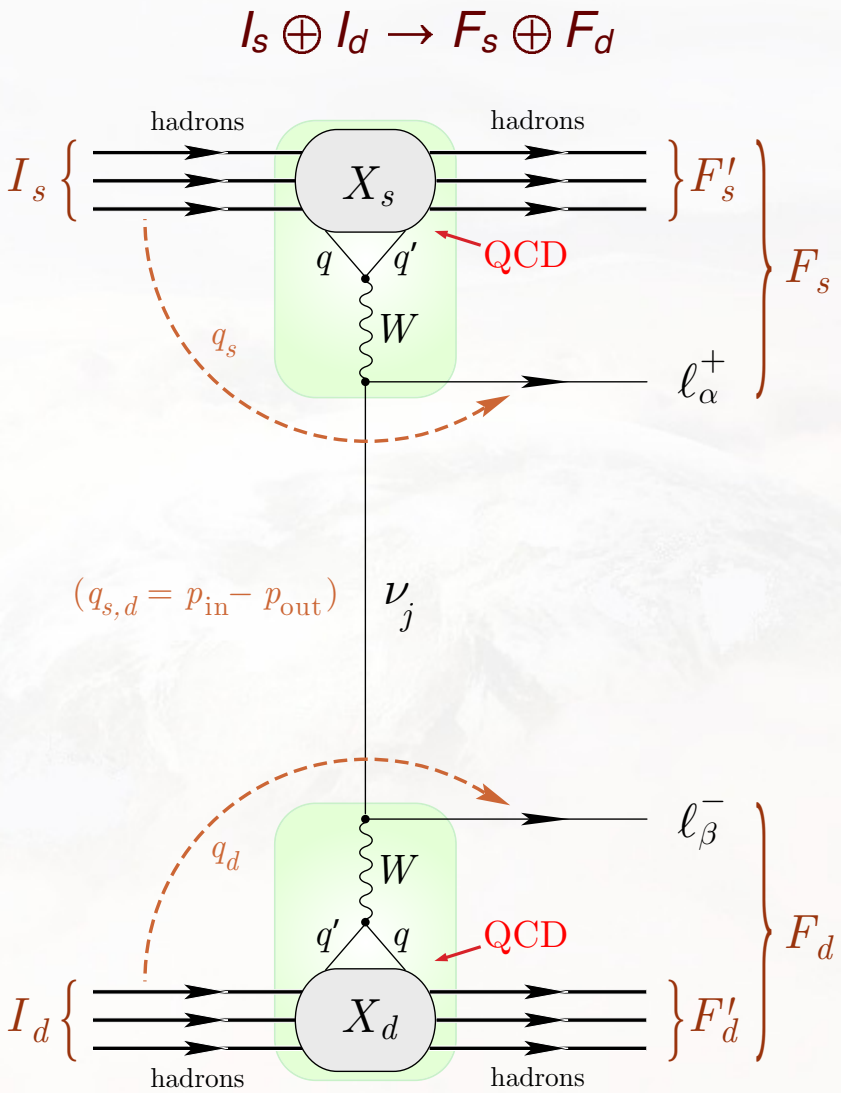

Properties of the function $\phi(\boldsymbol{k}, \boldsymbol{p})$

- $\phi(\boldsymbol{k}, \boldsymbol{p})$ must be a Lorentz-invariant due to the fact that the wave packets states must transform at the same way as the plane-wave states under the Lorentz transformation

$$|\boldsymbol{p}, s, x\rangle \longmapsto U_\Lambda |\boldsymbol{p}, s, x\rangle = |\boldsymbol{p}', s, x'\rangle.$$

- Function $\phi(\boldsymbol{k}, \boldsymbol{p})$ is supposed to have a sharp peak in point $\boldsymbol{k} = \boldsymbol{p}$.
- The sharpness of the peak is governed by the small parameter σ.

- The wave packet state is supposed to satisfy the correspondence principle:

$$\lim_{\sigma \to 0} |\boldsymbol{p}, s, x\rangle = |\boldsymbol{p}, s\rangle, \quad \lim_{\sigma \to 0} \phi(\boldsymbol{k}, \boldsymbol{p}) = (2\pi)^3 2E_{\boldsymbol{p}} \delta(\boldsymbol{k} - \boldsymbol{p}).$$

Coordinate representation

- The QFT field operator:

$$\Psi(x) = \int \frac{d\boldsymbol{k}}{(2\pi)^3\sqrt{2E_{\boldsymbol{k}}}} \sum_s \left[a_{\boldsymbol{k}s} u_s(\boldsymbol{k}) e^{-ikx} + b^\dagger_{\boldsymbol{k}s} v_s(\boldsymbol{k}) e^{ikx} \right].$$

- The quantity

$$\langle 0|\Psi(x)|\boldsymbol{p}, s\rangle = u_s(\boldsymbol{p}) e^{-ipx}$$

  can be considered as a coordinate representation of the plane wave state.

- Analogously, one can came to the conclusion that the coordinate representation of the wave packet state should have the form:

$$\langle 0|\Psi(x)|\boldsymbol{p}, s, y\rangle \approx e^{-ipy} u_s(\boldsymbol{p}) \psi(\boldsymbol{p}, y - x),$$

$$\psi(\boldsymbol{p}, x) = \int \frac{d\boldsymbol{k}}{(2\pi)^3 2E_{\boldsymbol{k}}} \phi(\boldsymbol{k}, \boldsymbol{p}) e^{ikx}.$$

Contracted Relativistic Gaussian Packet model

Wave function of the CRGP wave packet in the momentum representation is defined as:

$$\phi(\boldsymbol{k}, \boldsymbol{p}) = \frac{2\pi^{3/2}}{\sigma^2} \frac{m}{\sigma} \exp\left[\frac{(k-p)^2}{4\sigma^2}\right].$$

Model is valid under the following conditions:

$$(px)^2 \ll m^4/\sigma^4, \qquad (px)^2 - m^2x^2 \ll m^4/\sigma^4, \qquad \sigma^2 \ll m^2.$$

It than follows that the wave function describing the wave packet in the coordinate representation is

$$\psi(\boldsymbol{p}, x) = \exp\left(imx^0_\star - \sigma^2 \boldsymbol{x}^2_\star\right) = \exp\left\{i(px) - \frac{\sigma^2}{m^2}\left[(px)^2 - m^2x^2\right]\right\}.$$

$$P_{\alpha\beta}(L,E) = \sum_{ij} V^*_{\alpha i} V_{\alpha j} V^*_{\beta j} V_{\beta i} \exp\left(i\varphi_{ij} - \mathscr{A}_{ij}^2 - \mathscr{B}_{ij}^2\right), \tag{12}$$

$$\varphi_{ij} = \frac{2\pi L}{L_{ij}}, \qquad L_{ij} = \frac{4\pi E_\nu}{\Delta m^2_{ij}}, \qquad \Delta m^2_{ij} = m^2_i - m^2_j, \qquad \Delta E_{ij} = E_i - E_j.$$

$$\mathscr{A}_{ij} = \frac{2\pi \mathfrak{D} L}{E_\nu L_{ij}}, \qquad \mathscr{B}_{ij} = \frac{\Delta E_{ji}}{4\mathfrak{D}}. \tag{13}$$

- $\mathfrak{D}$ is the neutrino energy uncertainty, $\mathfrak{D} \ll E_\nu$.
- The additional factor $\exp\left(-\mathscr{A}_{ij}^2\right)$ suppresses the interference between the different neutrino types if the distance between the neutron source and detector exceeds the ”coherence length“:

$$L^{\rm coh}_{ij} = 1/(\Delta v_{ij}\mathfrak{D}) \gg |L_{ij}| \qquad (\Delta v_{ij} = |v_j - v_i|),$$

- The additional factor $\exp\left(-\mathscr{B}_{ij}^2\right)$ suppresses the interference if the neutrino wave packets are extremely delocalized in the space.

LO correction in the CRGP approximation

Back

The physical leading-order ISLV correction written in its most general form is very complicated. Let's consider it within the simple CRGP model for the external (in and out) wave packets. In this case, by using the 3rd order saddle-point asymptotic expansion for the integration in q_0, we obtain[20]

$$\mathfrak{C}_1 = -\frac{E_\nu^2}{\sigma_{\text{eff}}^4}, \qquad \frac{1}{\sigma_{\text{eff}}^4} = \frac{1}{8}\left[\rho^2 - \frac{2\kappa}{r} + \frac{\left(\upsilon_1^2 + \upsilon_2^2\right)^2}{r^2}\right] > 0, \tag{14}$$

where

$$r = \widetilde{\Re}_{00} - 2\widetilde{\Re}_{03} + \widetilde{\Re}_{33}, \qquad \kappa = \upsilon_1^2\widetilde{\Re}_{11} + 2\upsilon_1\upsilon_2\widetilde{\Re}_{12} + \upsilon_2^2\widetilde{\Re}_{22},$$
$$\rho^2 = \widetilde{\Re}_{11}^2 + 2\widetilde{\Re}_{12}^2 + \widetilde{\Re}_{22}^2, \qquad \upsilon_i = \widetilde{\Re}_{0i} - \widetilde{\Re}_{3i} \quad (i = 1, 2),$$

$$\widetilde{\Re}^{\mu\nu} = \widetilde{\Re}_s^{\mu\nu} + \widetilde{\Re}_d^{\mu\nu},$$

$\widetilde{\Re}_{s,d}^{\mu\nu}$ are the components of the inverse overlap tensors in the source and detector vertices.[21] The 3rd axis of the lab. frame is directed along the neutrino velocity.

[20] Negativity of $\mathfrak{C}_1$ is probably a more general property. Note that $r = \widetilde{\Re}^{\mu\nu} l^\mu l^\nu = \text{inv}$.

[21] Exact formulas for $\widetilde{\Re}_{s,d}^{\mu\nu}$ are derived in Ref. [NS-2013].

Cosmological constrains on number of neutrino types

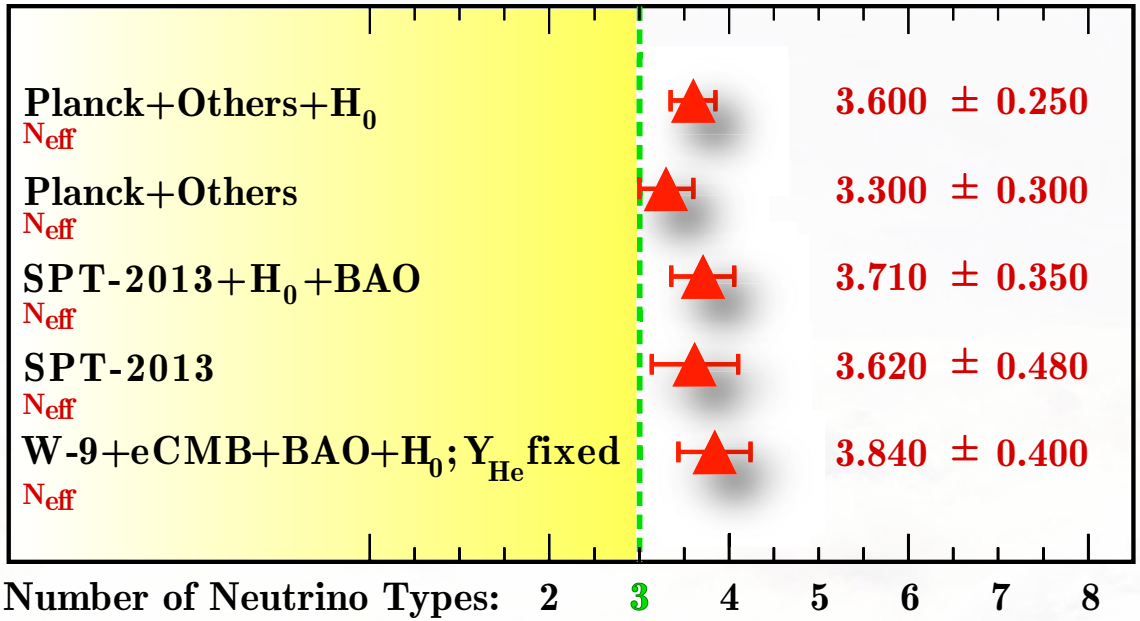

Constraints obtained on the number of effective neutrino species $N_{\rm eff}$ from different cosmological observables, based on WMAP 9-year data, *Planck*, SPT, BAO, and Hubble constant astrophysical inputs.[22]

$$\left.\begin{array}{r} N_{\rm eff} < 3.80 \\ m^{\rm eff}_{\nu,\rm sterile} < 0.42\ {\rm eV} \end{array}\right\}$$ 95% C.L.; *Planck*+W-9+high-ℓ+BAO for $m^{\rm thermal}_{\nu,\rm sterile} < 10$ eV.

One species of $\nu_{\rm sterile}$ with $m_4 \lesssim 1$ eV can be **marginally** accommodated by precision cosmological data. But two species with $m_4 \approx 1$ eV each, or one species with $m_4 \approx 2$ eV is still **strongly disfavored**.[23]

[22] See A. Gando *et al.* arXiv: 1312.0896 [physics.ins-det] and references therein.

[23] See K. N. Abazajian *et al.* arXiv: 1204.5379 [hep-ph] for a review. The latest results of the *Planck* experiment are reported in P.A.R. Ade *et al.* arXiv: 1303.5076 [astro-ph.CO].

Extra data on N_{eff}

Observations have hinted at the $(1-2)\sigma$ level for $N_{eff} > N_{eff}^{SM} = 3.046$.
Various (non-independent) measurements:

- **CMB alone:**
  - 3.55 ± 0.60 (WMAP9 + eCMB + BAO + H_0) arXiv:1212.5226
  - 3.50 ± 0.47 (SPT + CMB + BAO + H_0) arXiv:1212.6267
  - 2.87 ± 0.60 (WMAP7 + ACT + BAO+ H_0) arXiv:1301.0824
  - 3.30 ± 0.27 (Planck + eCMB + BAO + H_0) arXiv:1303.5076
- **CMB + H_0:**
  - 3.84 ± 0.40 (WMAP9 + eCMB + BAO + H_0) arXiv:1212.5226
  - 3.71 ± 0.35 (SPT + CMB + BAO + H_0) arXiv:1212.6267
  - 3.52 ± 0.39 (WMAP7 + ACT + BAO+ H_0) arXiv:1301.0824
  - 3.62 ± 0.25 (Planck + eCMB + BAO + H_0) arXiv:1303.5076

Current & future VSBL experiments

Experiment	**Reactor**	**Power** (MW_{th})	**Baseline** (m)
Angra Neutrino Project (Brazil)	Angra II	4000	∼30
Nucifer (CEA-Saclay, France)	Osiris rr	70	7
Stereo (ILL, Grenoble, France)	ILL rr	58.3	7–9
SOLID/MARS (ILL, Grenoble, France)	ILL rr	58.3	8
JOYO (Japan)	Jōyō rr	140	24.3
HANARO-4 (Korea)	HANARO rr	30	6
Neutrino-4 (Dimitrovgrad, Russia)	SM-3 rr	100	6–12 (5–13.5)
DANSS (Kalinin, ITEP-JINR, Russia)	KNPP	3000	9.7–12.2 (to 18.8)
DANSSino (prototype)			11
POSEIDON (PIK, Gatchina, Russia)	PIK rr	100	5–15
ATR (INL, Idaho, USA)	ATR rr	120 (150)	9.5–12.5 (12–30)
HFIR (ORNL, USA)	HFIR rr	85	3(?), 6.7–18
NBSR (Washington DC, USA) (?)	NBSR/NIST rr	20	3.9–15.5
miniTimeCube (Washington DC, USA)	NBSR/NIST rr	20	3.4–20
SCRAMM (Idaho, USA)	ATR rr	150	10–15
~~**SCRAAM** (San-Onofre, CA, USA)~~	San-Onofre	3000	24
~~**SONGS** (San Onofre, CA, USA)~~	San-Onofre	3438	24

SRP 1980[24]

TABLE II. Summary of results for the ratio $\langle\sigma_{\text{expt}}\rangle/\langle\sigma_{\text{theor}}\rangle$.

Distance from core center (m)	Reaction	Neutrino detection threshold (MeV)	Ratio AG spectrum	Ratio DVMS spectrum	Measured $\bar{\nu}_e$ spectrum (preliminary)
11.2	nc$d$	2.2	0.83 ± 0.13	1.10 ± 0.16	1.3[a] ± 0.22
11.2	cc$d$	4.0	0.32 ± 0.14	0.44 ± 0.19	0.61 ± 0.29
11.2	cc$p$	4.0	0.68 ± 0.12	0.88 ± 0.15	≡ 1.0
11.2	cc$p$	6.0	0.42 ± 0.09	0.58 ± 0.12	≡ 1.0
6	cc$p$	1.8	0.65 ± 0.09	0.84 ± 0.12	···
6	cc$p$	4.0	0.81 ± 0.11	1.02 ± 0.15	1.19 ± 0.27

[a] This number is uncertain because the $\bar{\nu}_e$ spectrum has thus far been measured > 4 MeV. If oscillations occur, the spectrum could be depressed below 4 MeV thus increasing this ratio.

[24] F. Reines, H. W. Sobel, and E. Pasierb. *Phys. Rev. Lett.* **45** (1980) 1307

From earlier analysis: Fits without ILL point

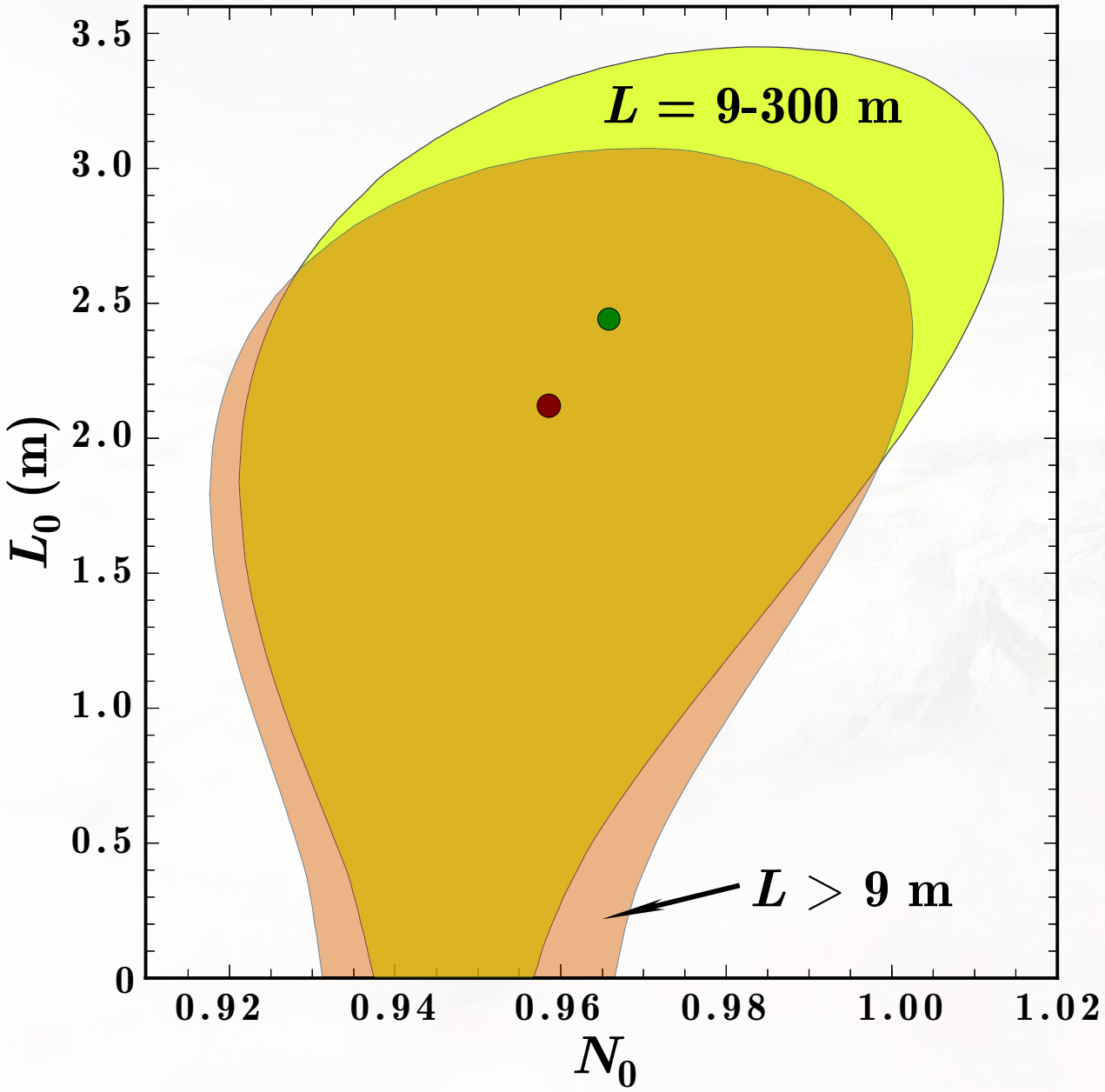

From earlier analysis: Error contours for different models

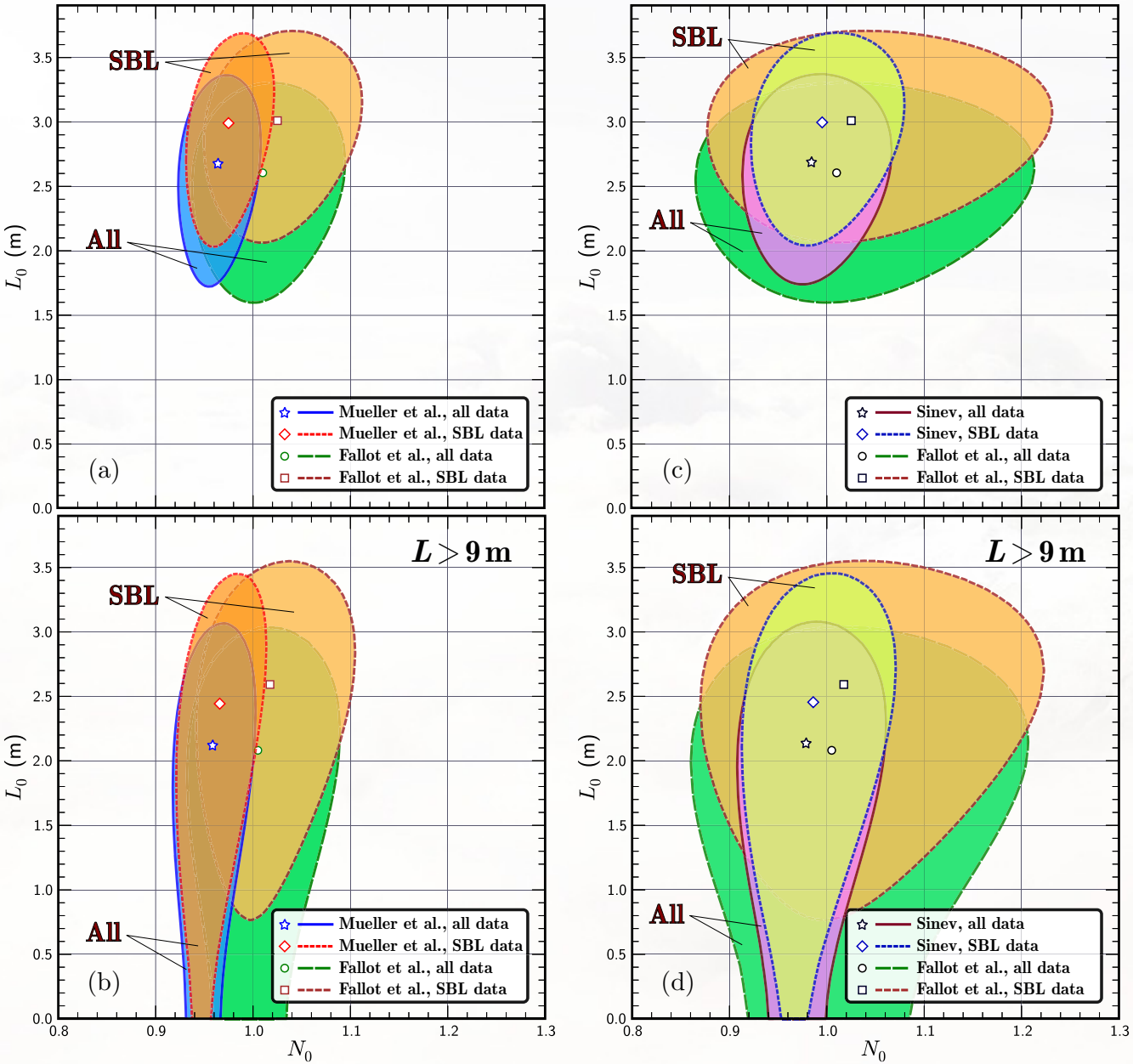

Spectra of Fallot *et al.* are taken from Ref. M. Fallot *et al. Phys. Rev. Lett.* **109** (2012) 202504. arXiv: 1208.3877 [nucl-ex].
Spectra of Sinev are taken from Ref. V. V. Sinev. *Yad. Fiz.* **76** (2013) 578. arXiv: 1207.6956 [nucl-ex].

Recall that in this and previous slides only the data published before 2017 were included in that fit.

Five-MeV excess

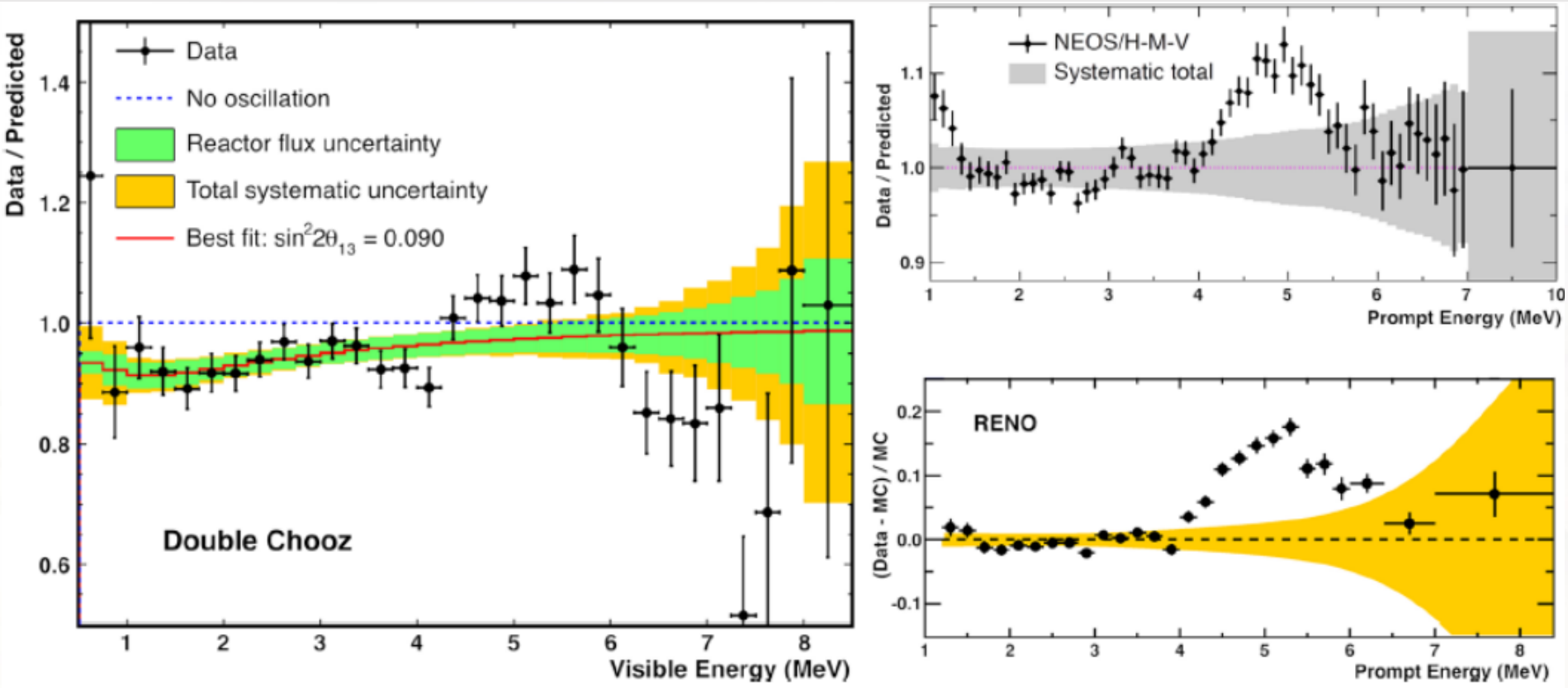

- Similar “bump” is seen also by Daya Bay and (erlier) by RONS (Rovno).
- This shape anomaly cannot be explained by detector effects or sterile neutrinos. Rather, it indicates the reactor model uncertainty is underestimated.[25]
- Fortunately, the impact of the bump to the extracted value of L_0 is marginal.

[25] Taken from a report by X. Qian, “Experimental overview of reactor neutrinos” (International Conference on Neutrinos and Dark Matter, ’NDM-2020’, Hurghada, January 11–14, 2020).

Expected signal from ν_4

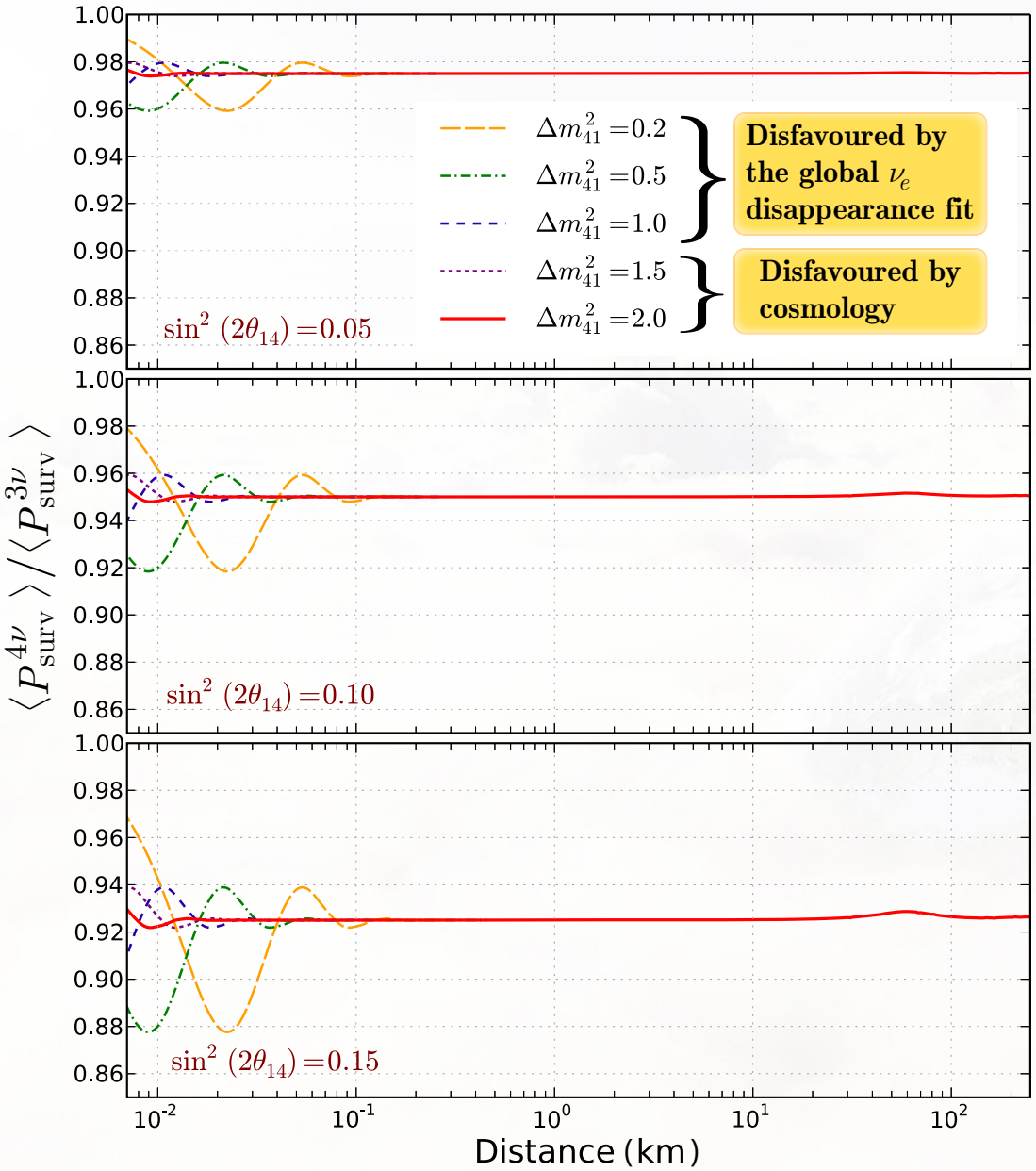

$$P^{4\nu}_{\rm surv} = 1 - \cos^4\theta_{14}\left(1 - P^{3\nu}_{\rm surv}\right) - \sin^2(2\theta_{14}) \times \left[\cos^2\theta_{13}\left(\cos^2\theta_{12}\sin^2\Delta_{41} + \sin^2\theta_{12}\sin^2\Delta_{42}\right) + \sin^2\theta_{13}\sin^2\Delta_{43}\right]$$

$$\simeq 1 - \cos^4\theta_{14}\left(1 - P^{3\nu}_{\rm surv}\right) - \sin^2(2\theta_{14})\sin^2\Delta_{41}.$$

The effect of a sterile neutrino with mass $m_4 \gtrsim 2$ eV is almost indistinguishable from the effect of renormalization of the $\overline{\nu}_e$ flux.

Comparison of models for $\overline{\nu}_e$ spectra

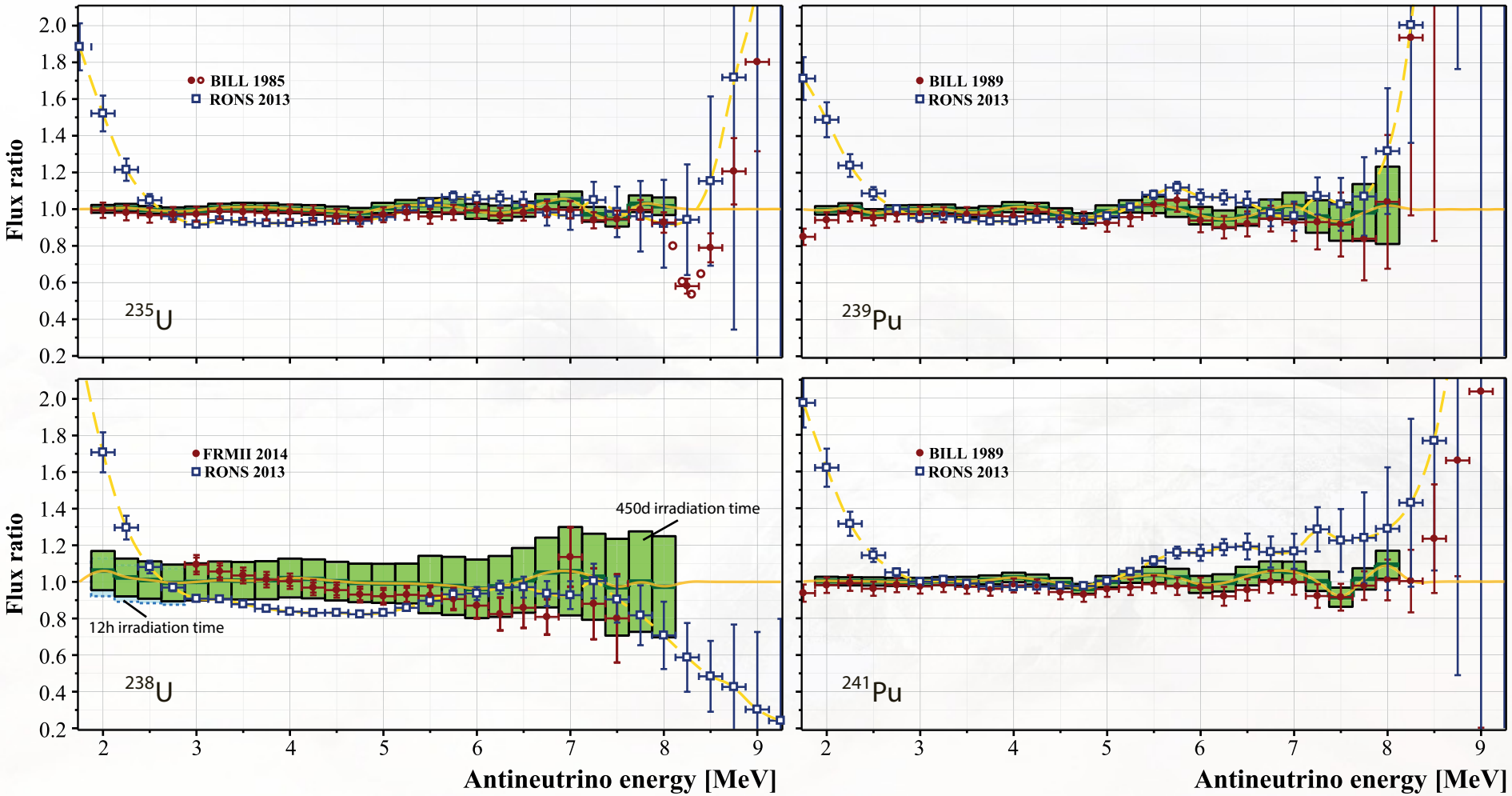

The same as in slides 25 and 26 but in another representation and in more detail.